LFU measurements of FCNC decays and anomalies in $b \to s\ell^+\ell^-$ transitions

Dan Moise

Implications of LHCb measurements and future prospects

27th October 2023

$b \to s\ell^+\ell^-$

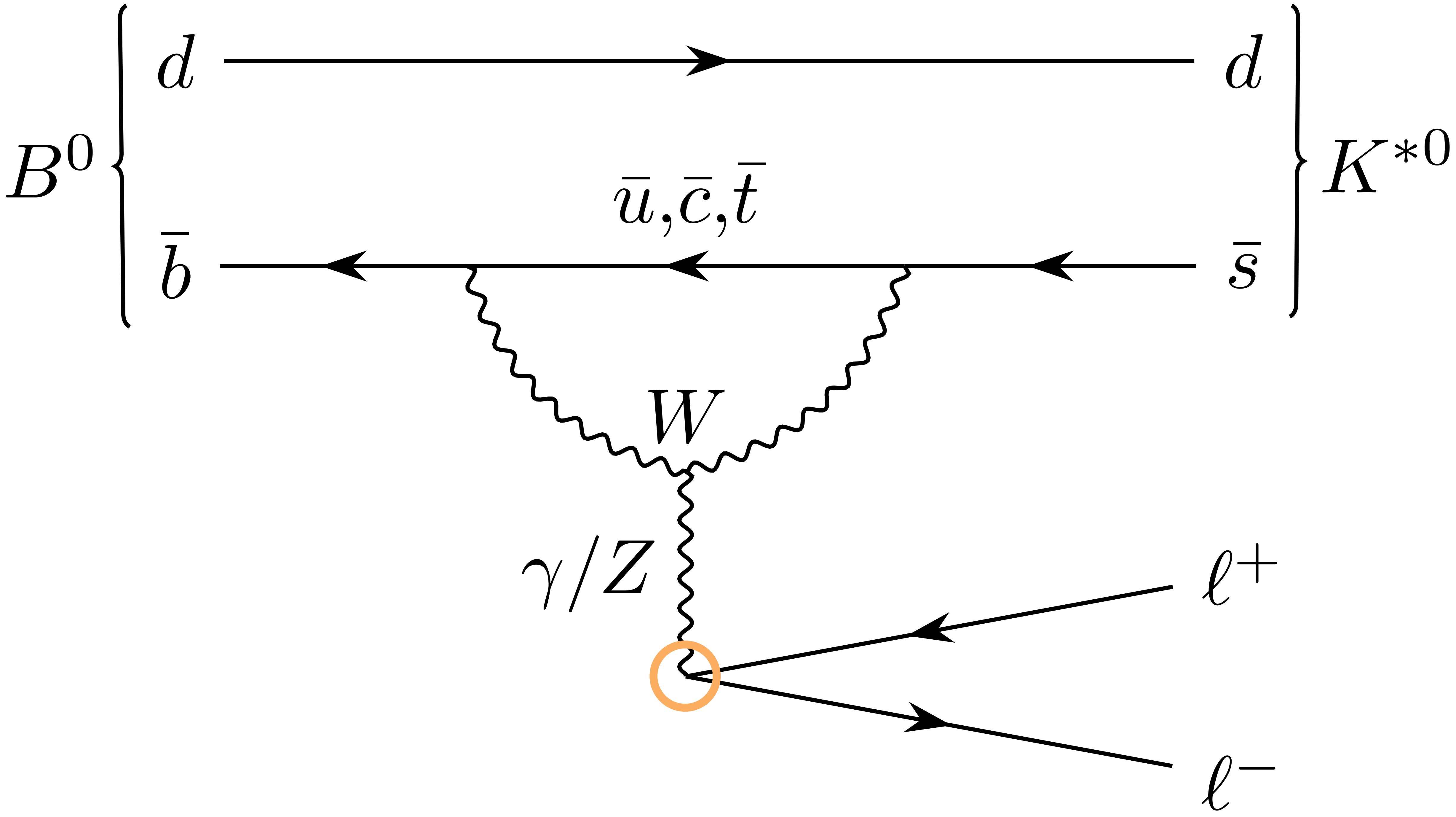

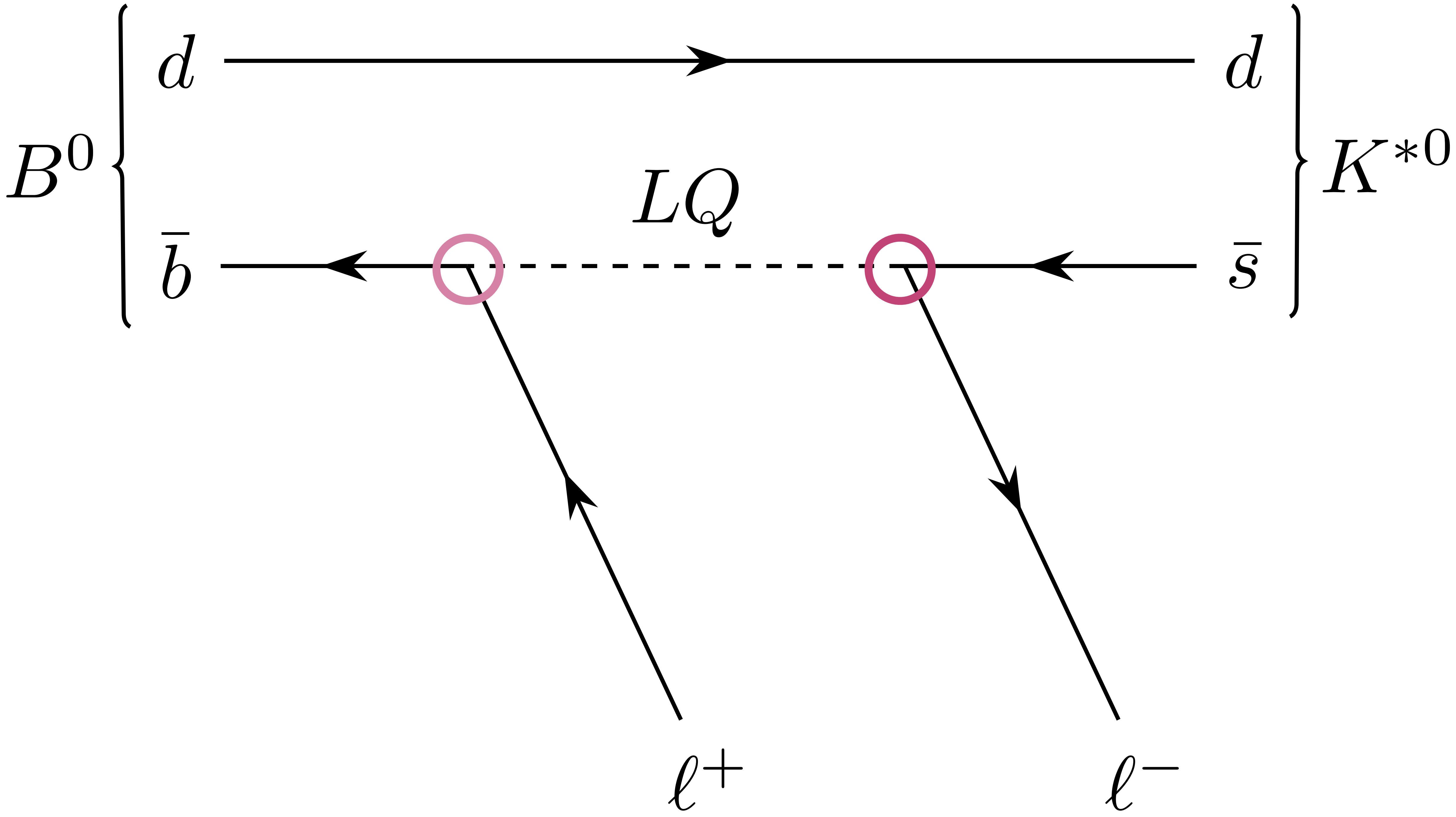

SM

- loop-suppressed (FCNC)
- universal couplings guaranteed

NP

- can enter at tree-level
- universal couplings not guaranteed

If NP at high mass scales

$$\mathcal{H}_{\text{eff}} \propto \Sigma_i C_i \mathcal{O}_i$$

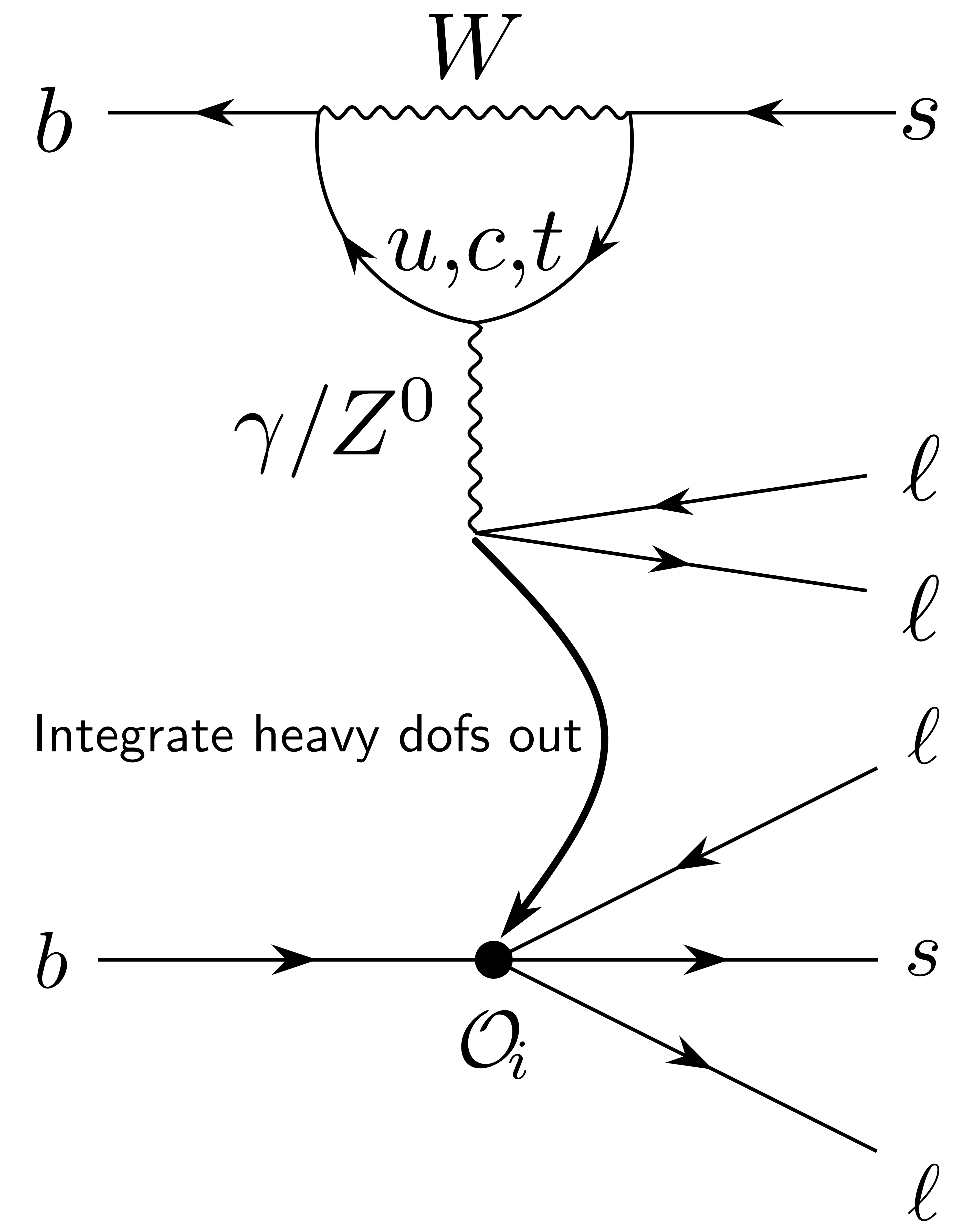

- local operators relevant at different $q^2 \equiv m^2(\ell^+\ell^-)$
- "effective coupling" coefficients may be affected by NP

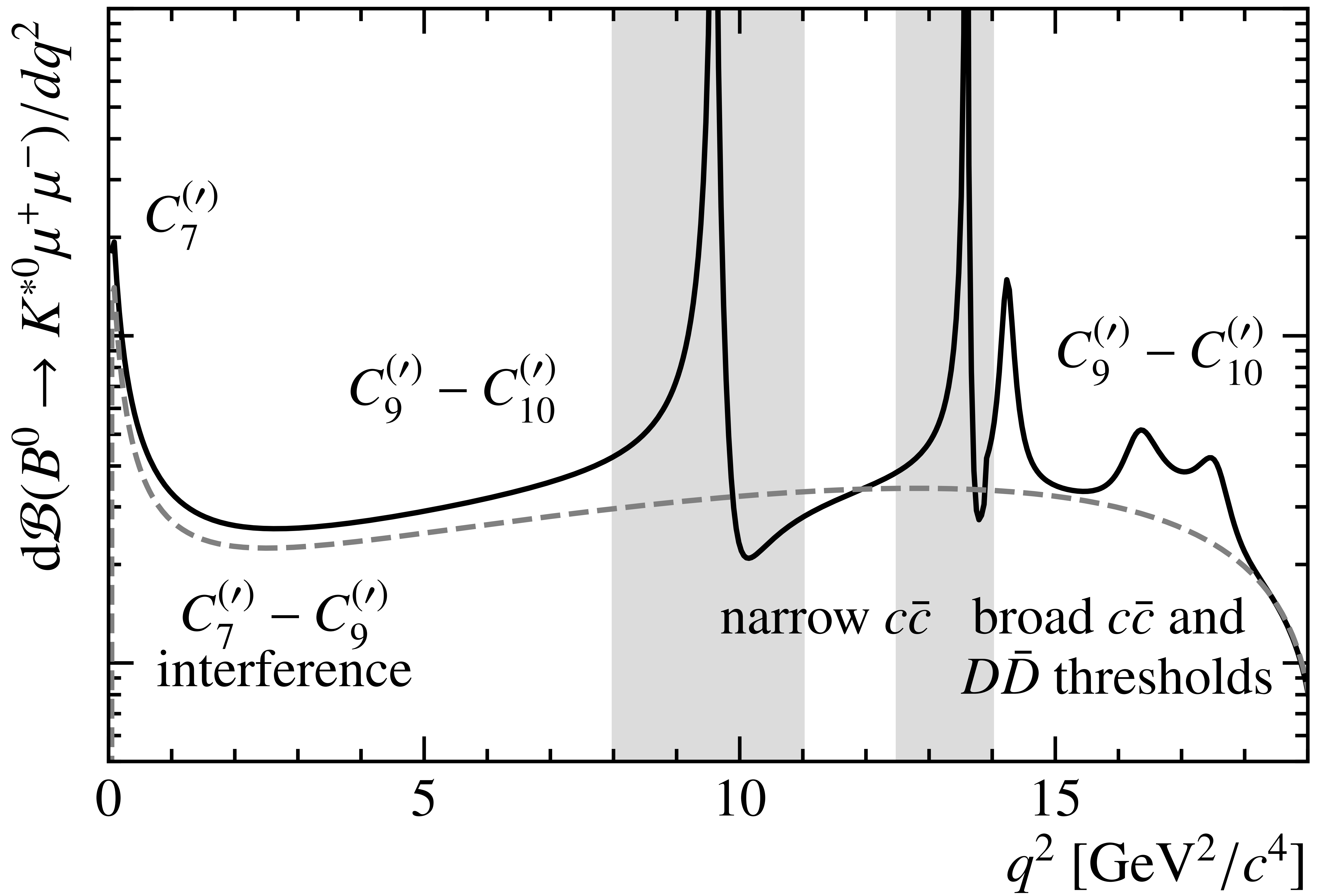

$$R_{H_s} \equiv \frac{\mathcal{B}(B^+ \to H_s \mu^+\mu^-)}{\mathcal{B}(B^+ \to H_s e^+e^-)} \bigg/ \frac{\mathcal{B}(B^+ \to H_s J/\psi(\to \mu^+\mu^-))}{\mathcal{B}(B^+ \to H_s J/\psi(\to e^+e^-))}$$

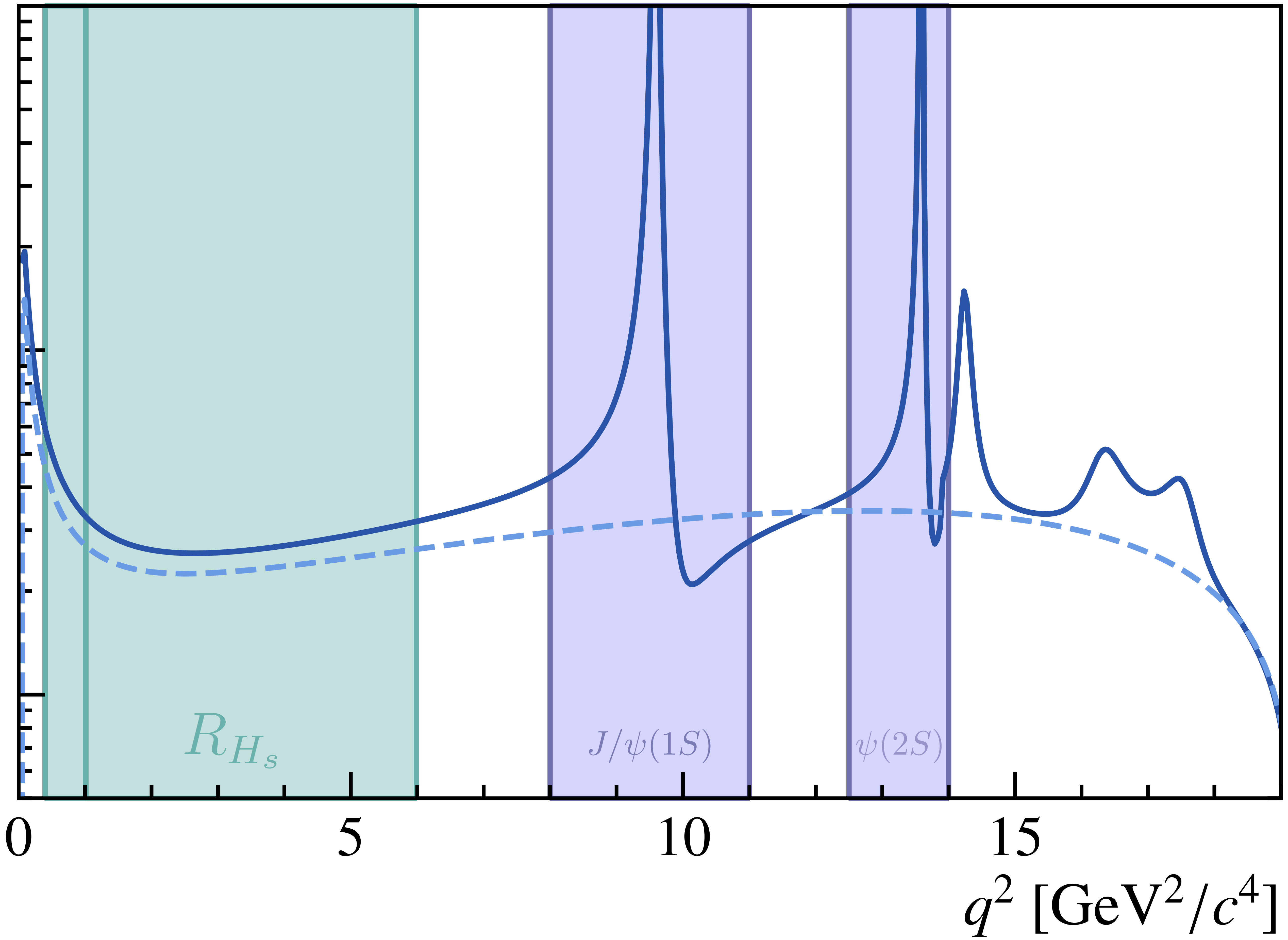

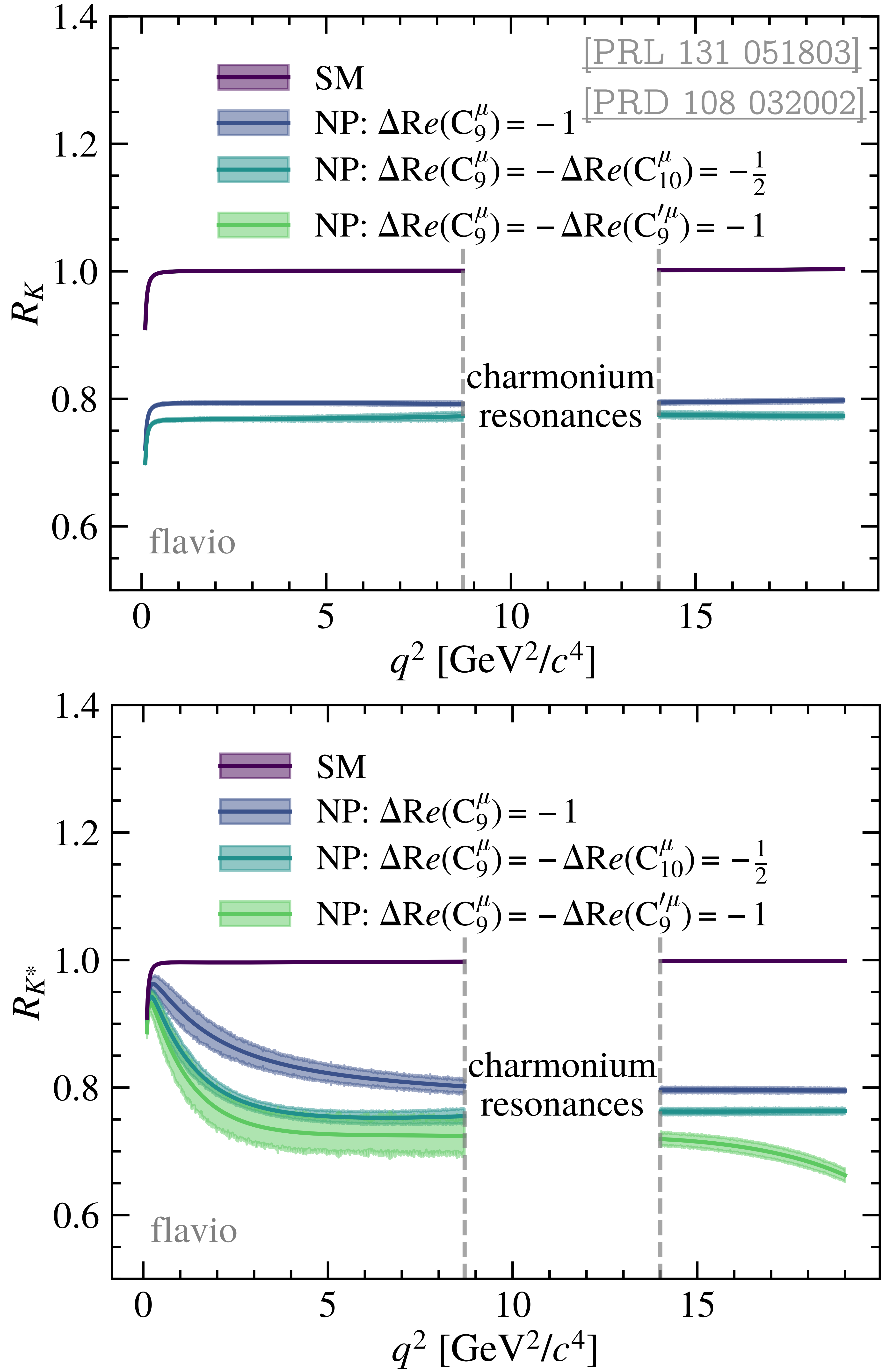

Electron-specific challenges

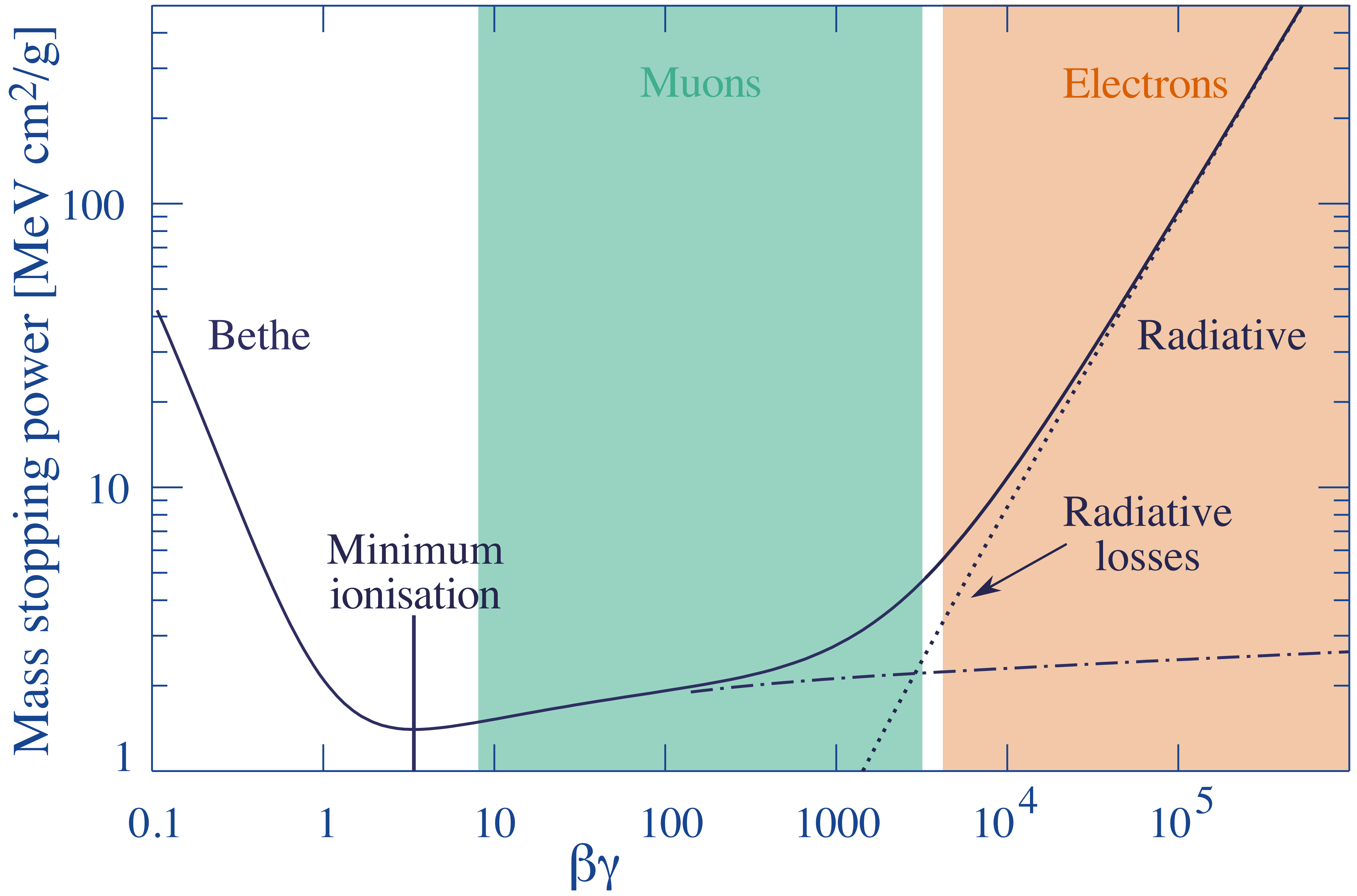

- large radiative losses
- tight L0 trigger thresholds

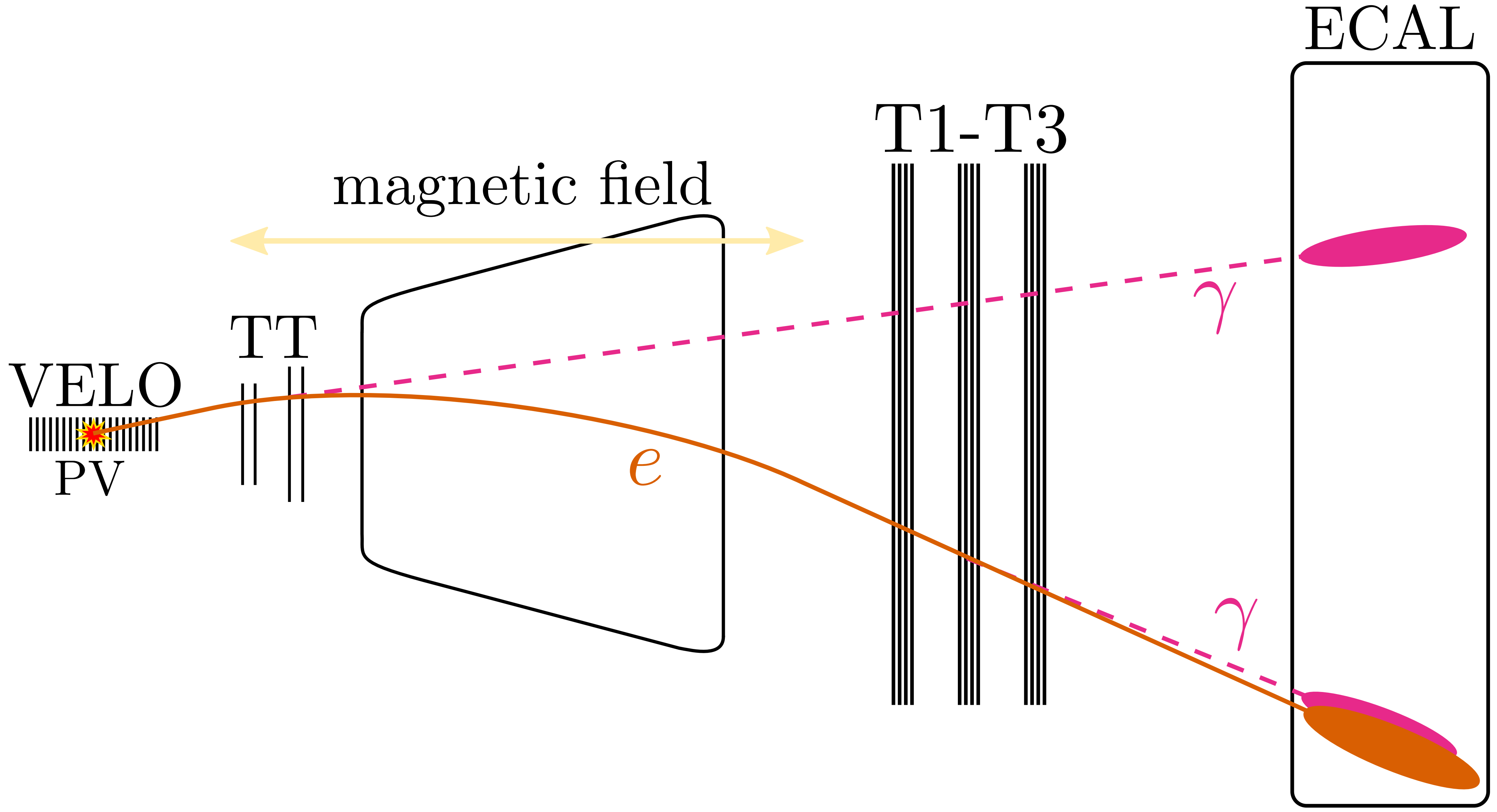

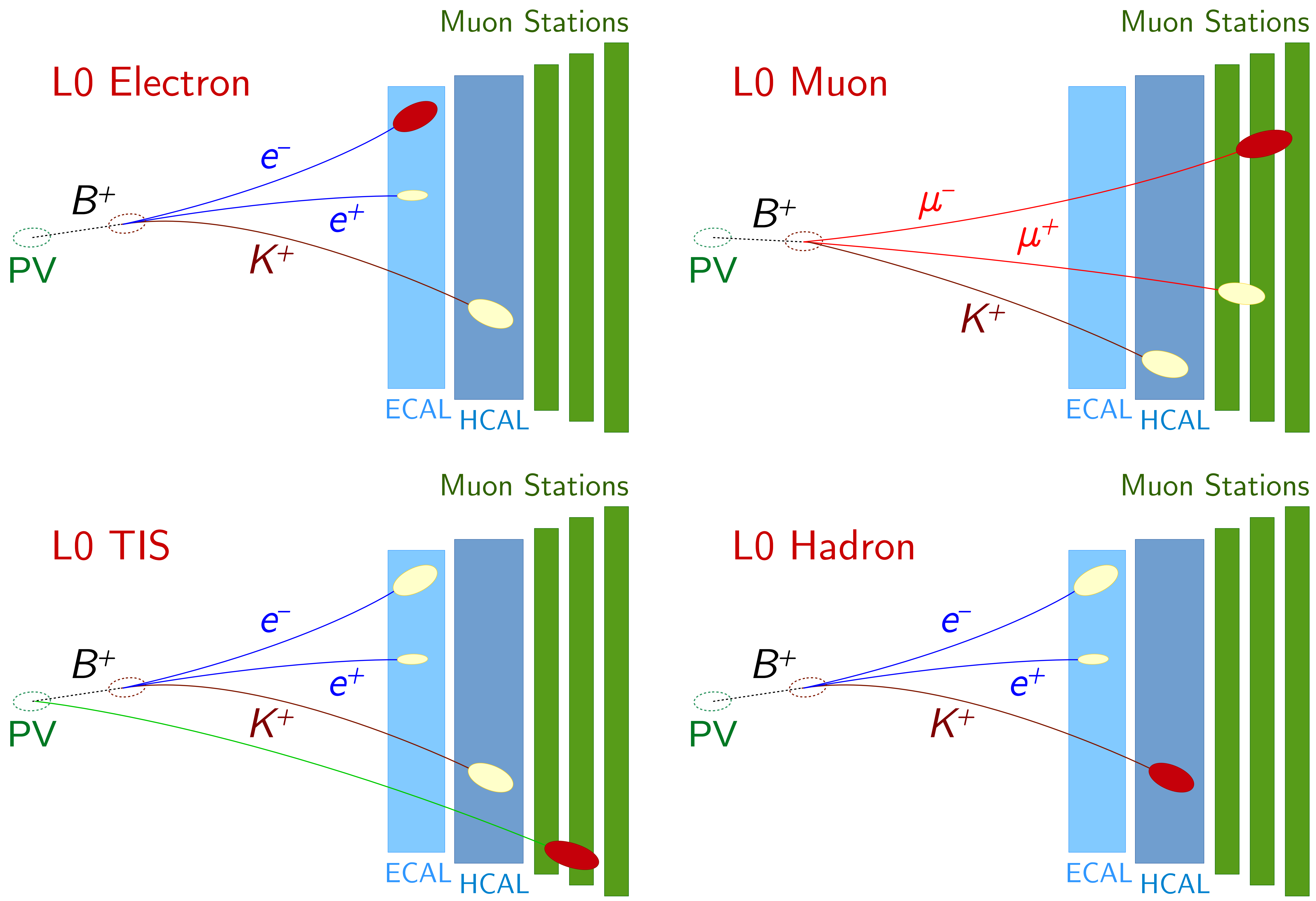

PRL 131 (2023) 051803

PRD 108 (2023) 032002

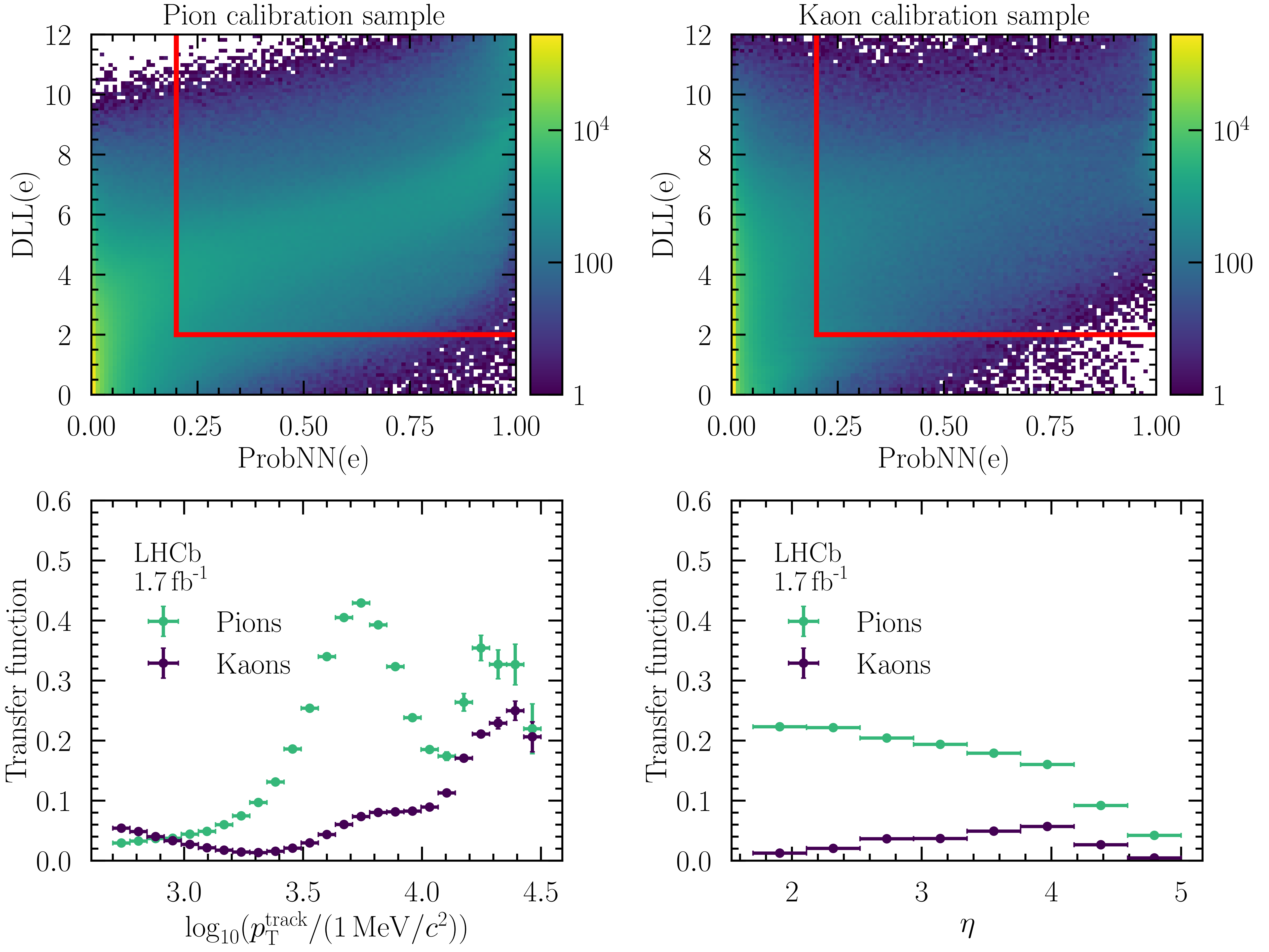

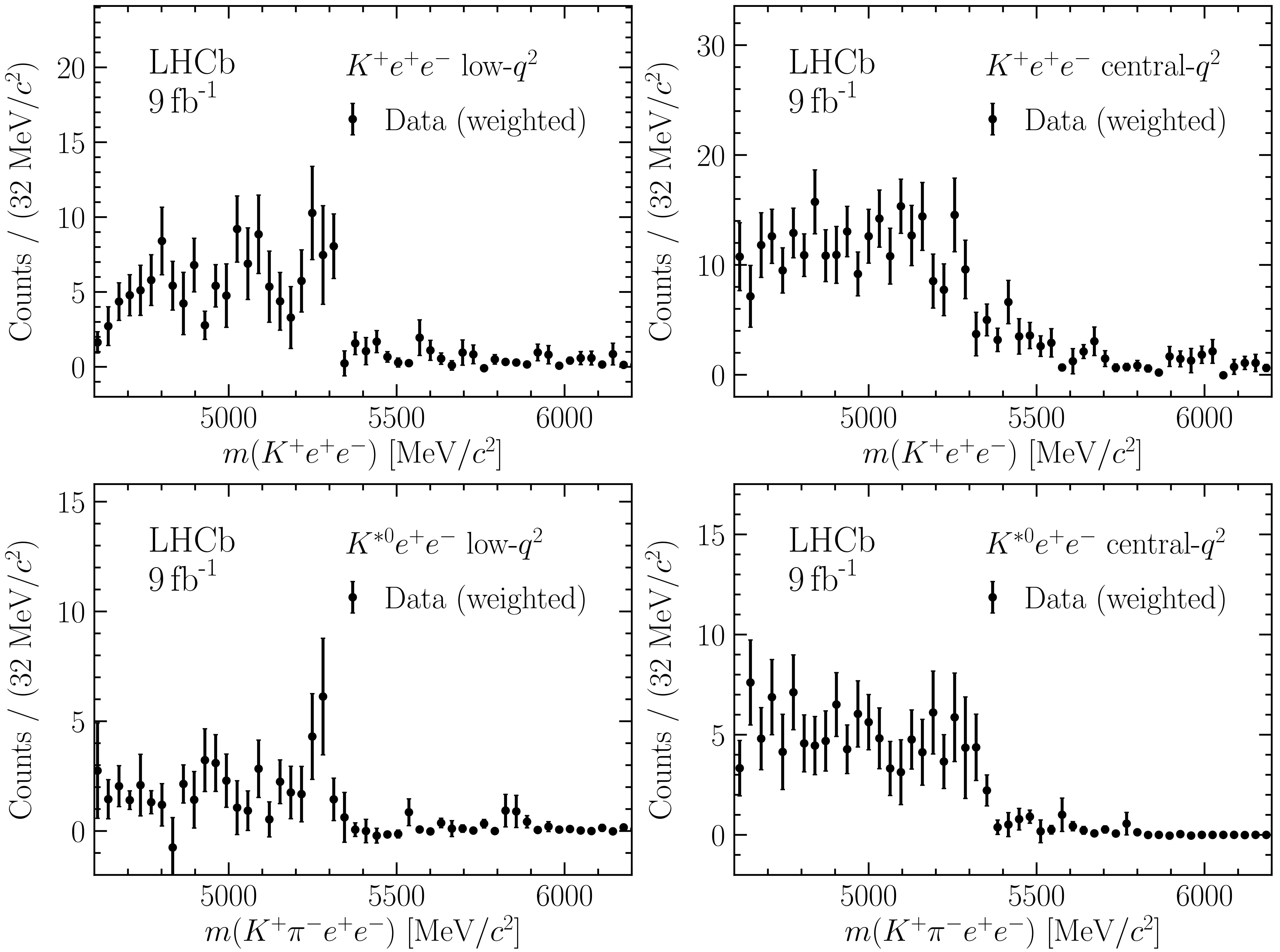

Latest measurements benefit from novel inclusive data-driven background estimation, stringent particle ID selection.

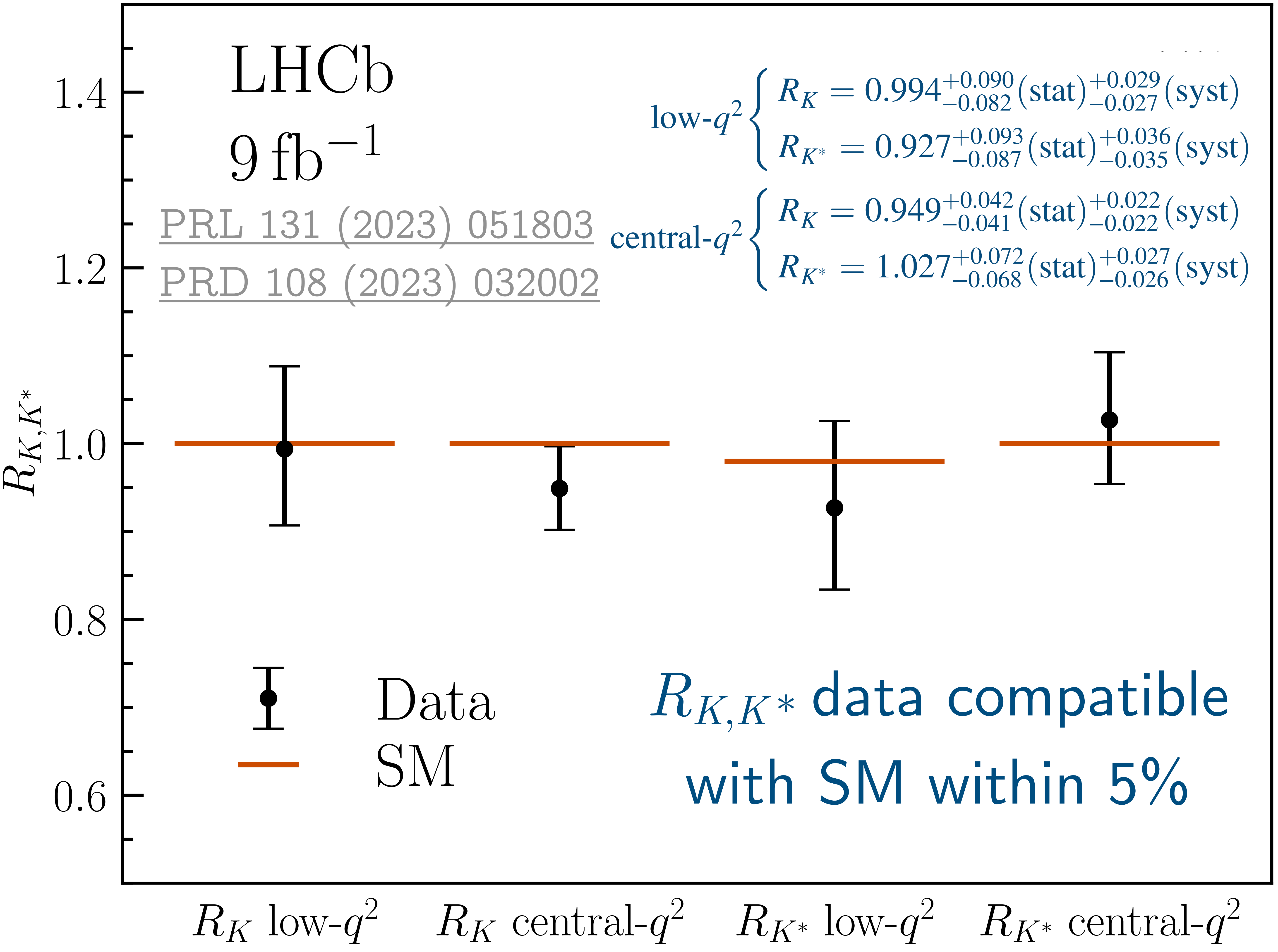

R_{H_s} precision bottleneck: statistics

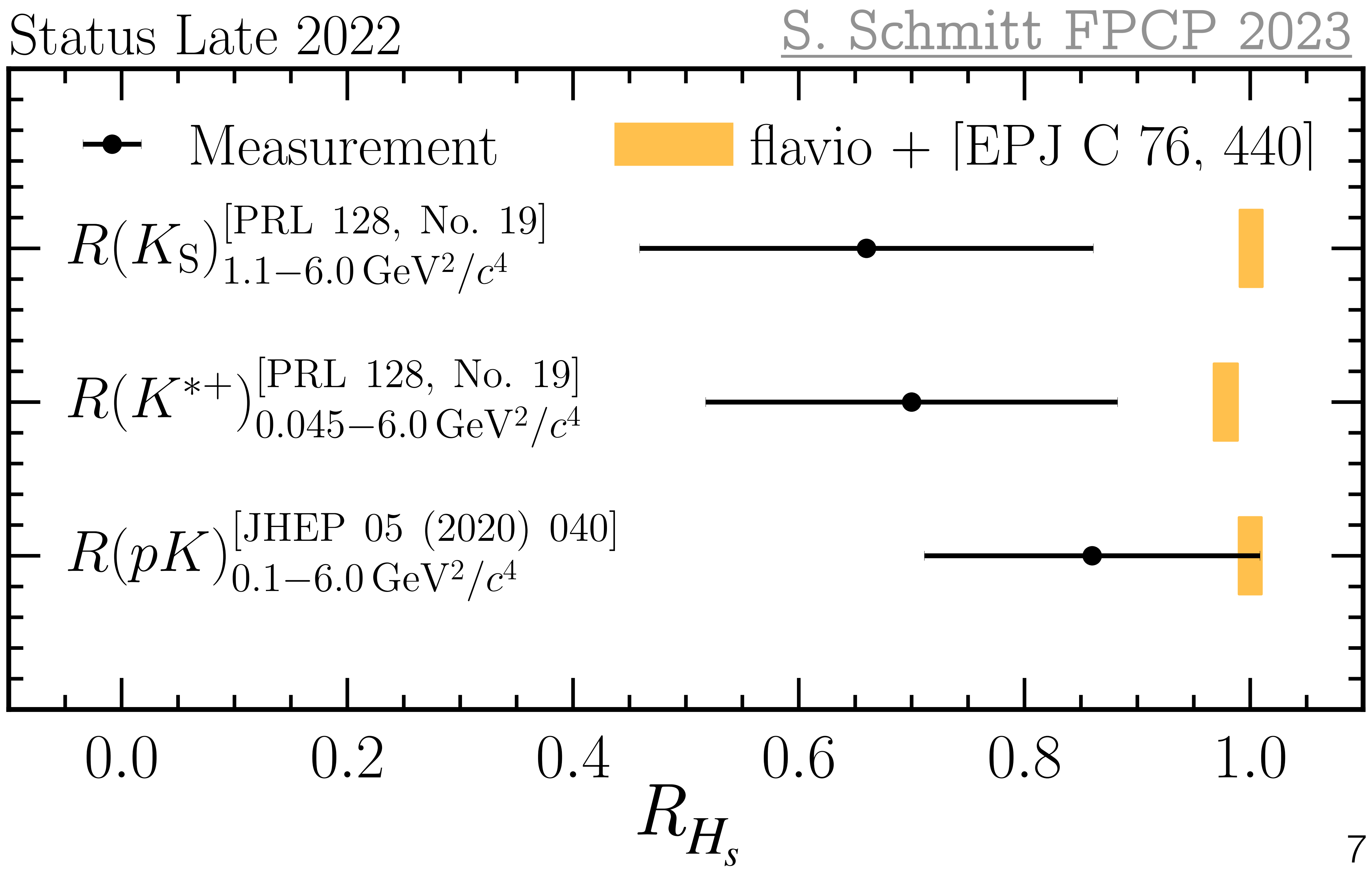

Measurements of $b \to s\mu^+\mu^-$ branching fractions systematically below SM predictions

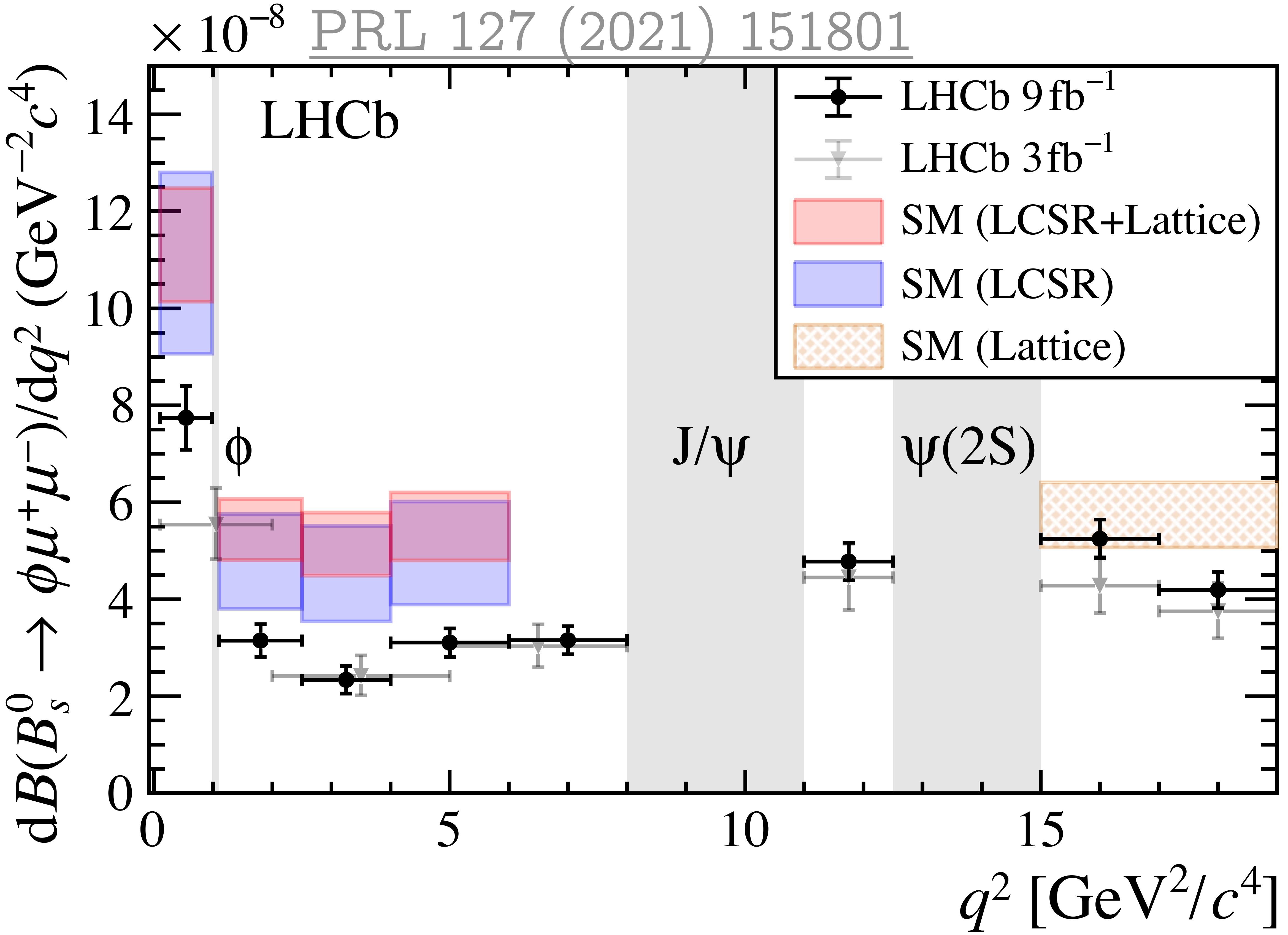

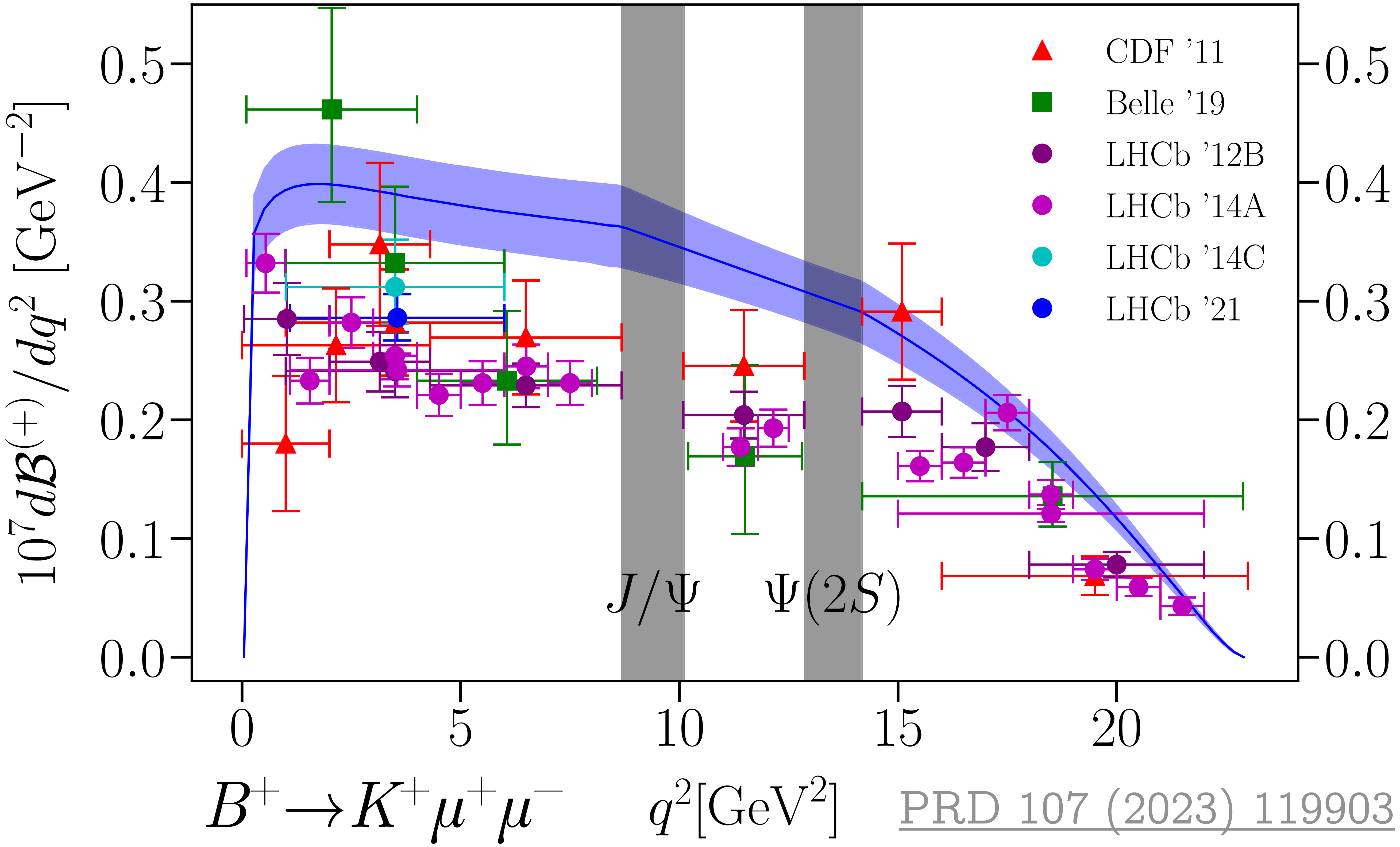

Data from angular binned angular analyses

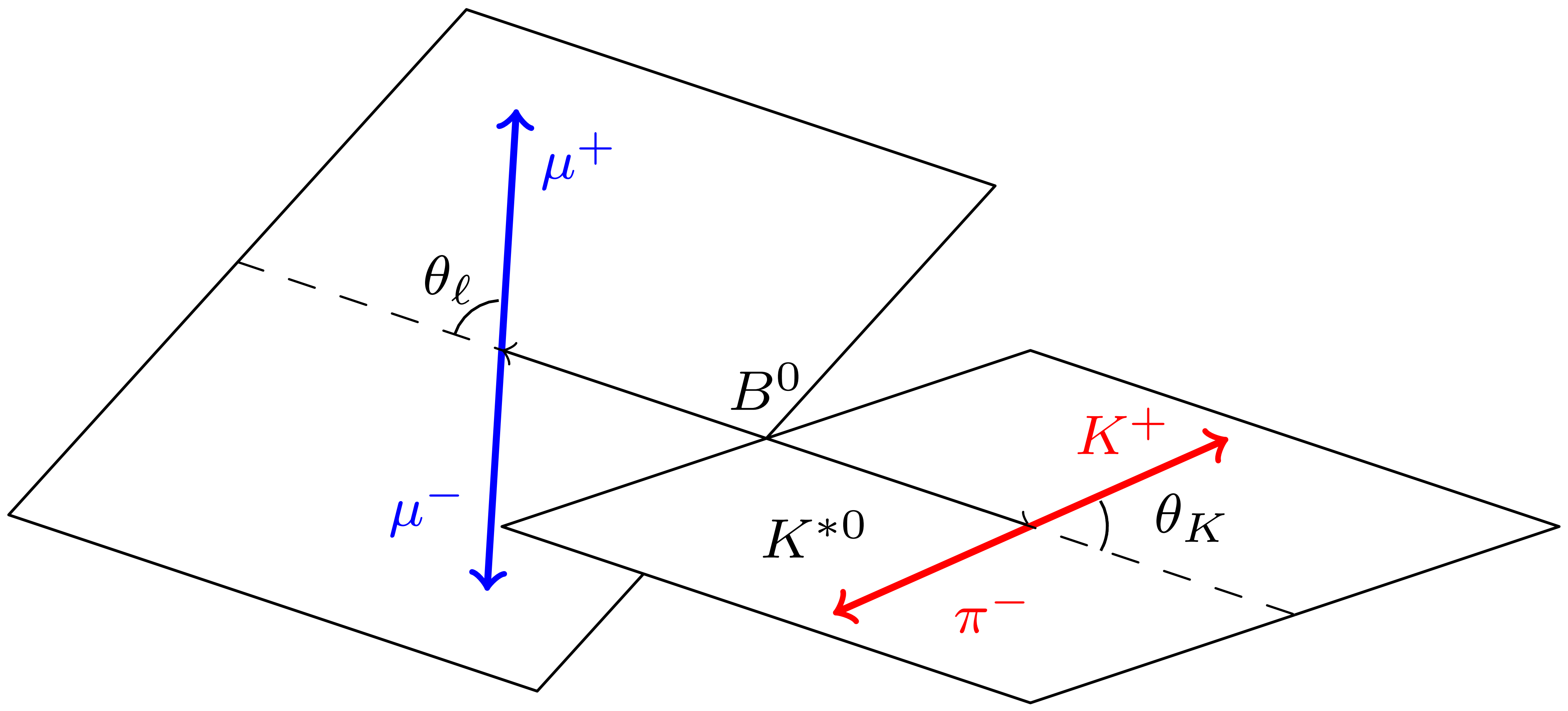

\+ stable and robust fits

− suboptimal statistical power

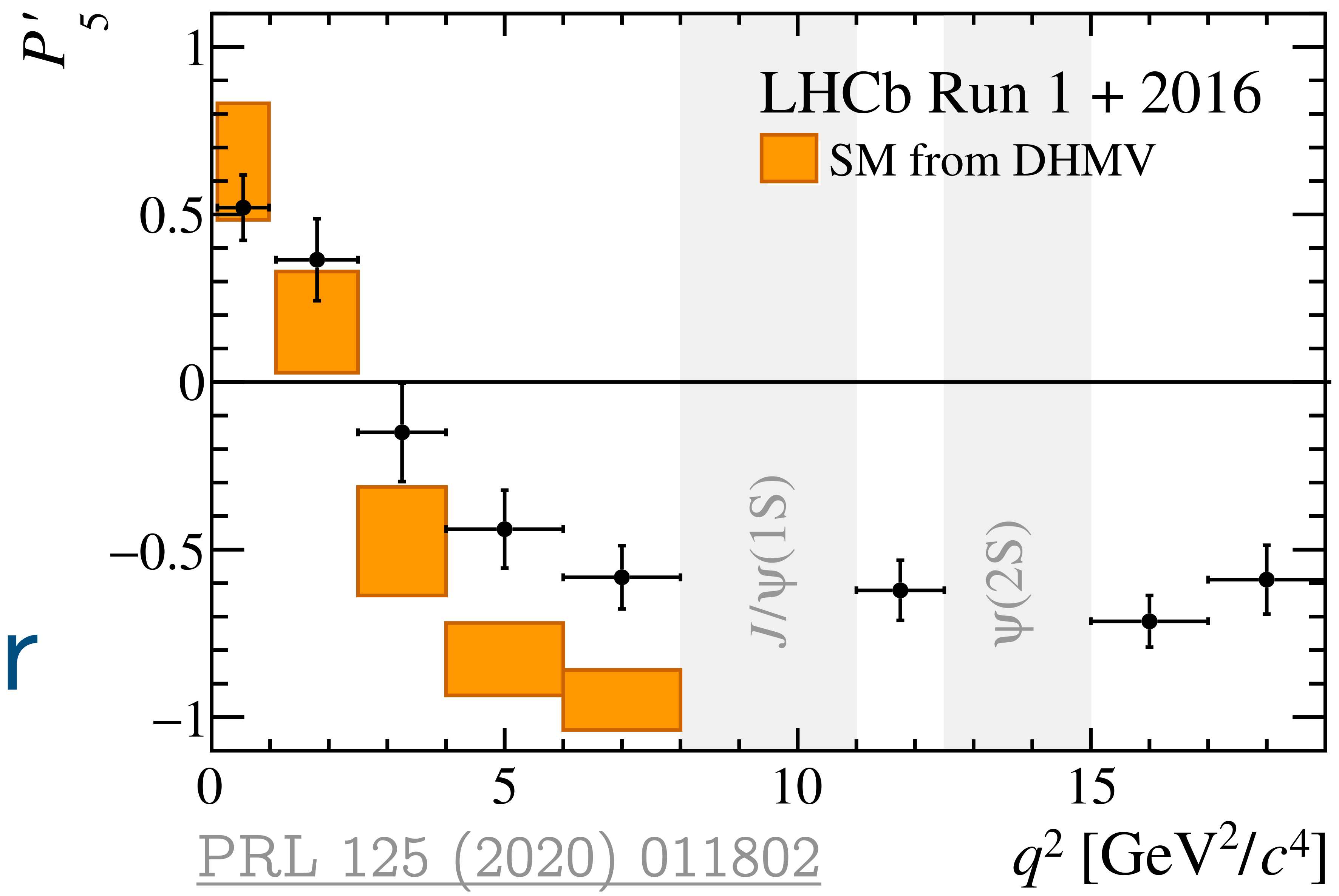

PRL 125 (2020) 011802

Data from angular binned angular analyses

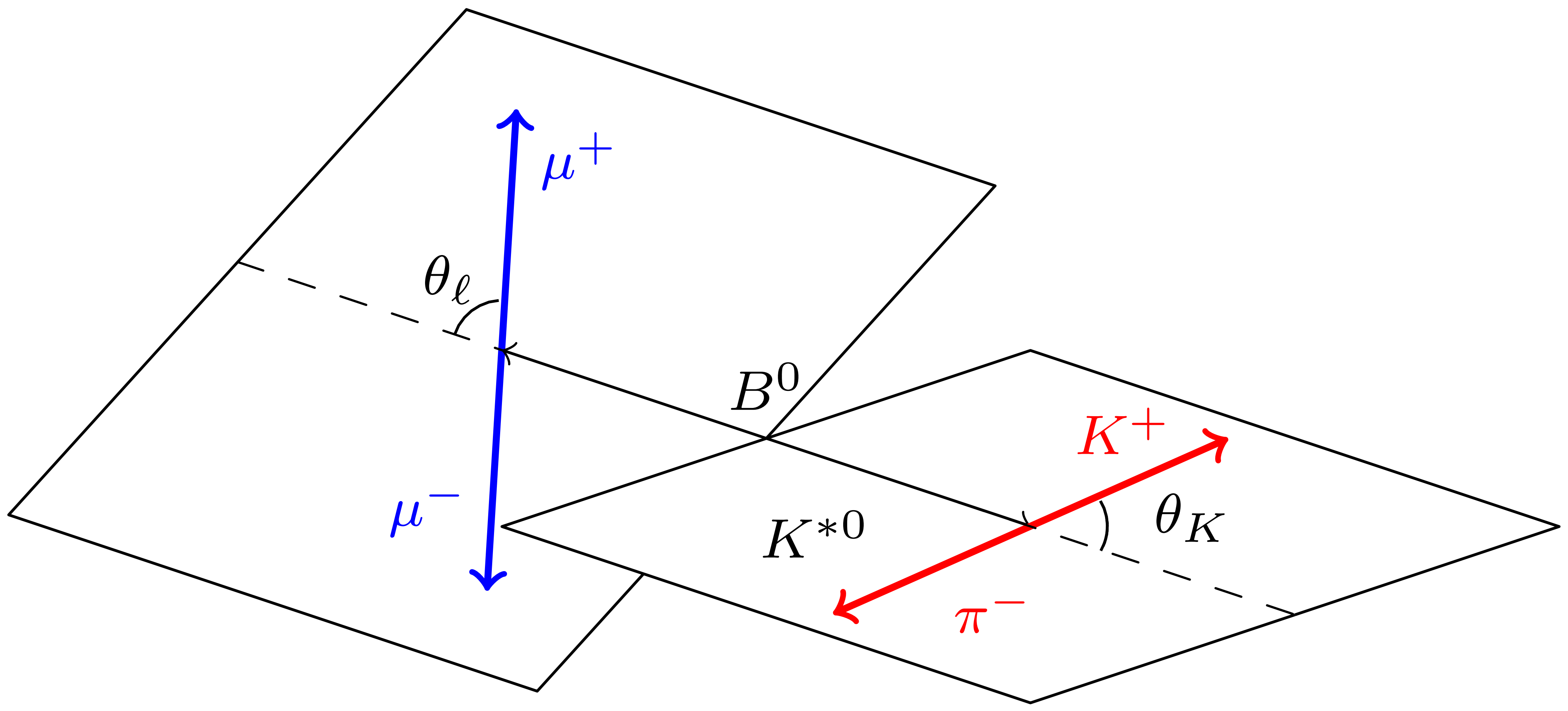

+ stable and robust fits
− suboptimal statistical power

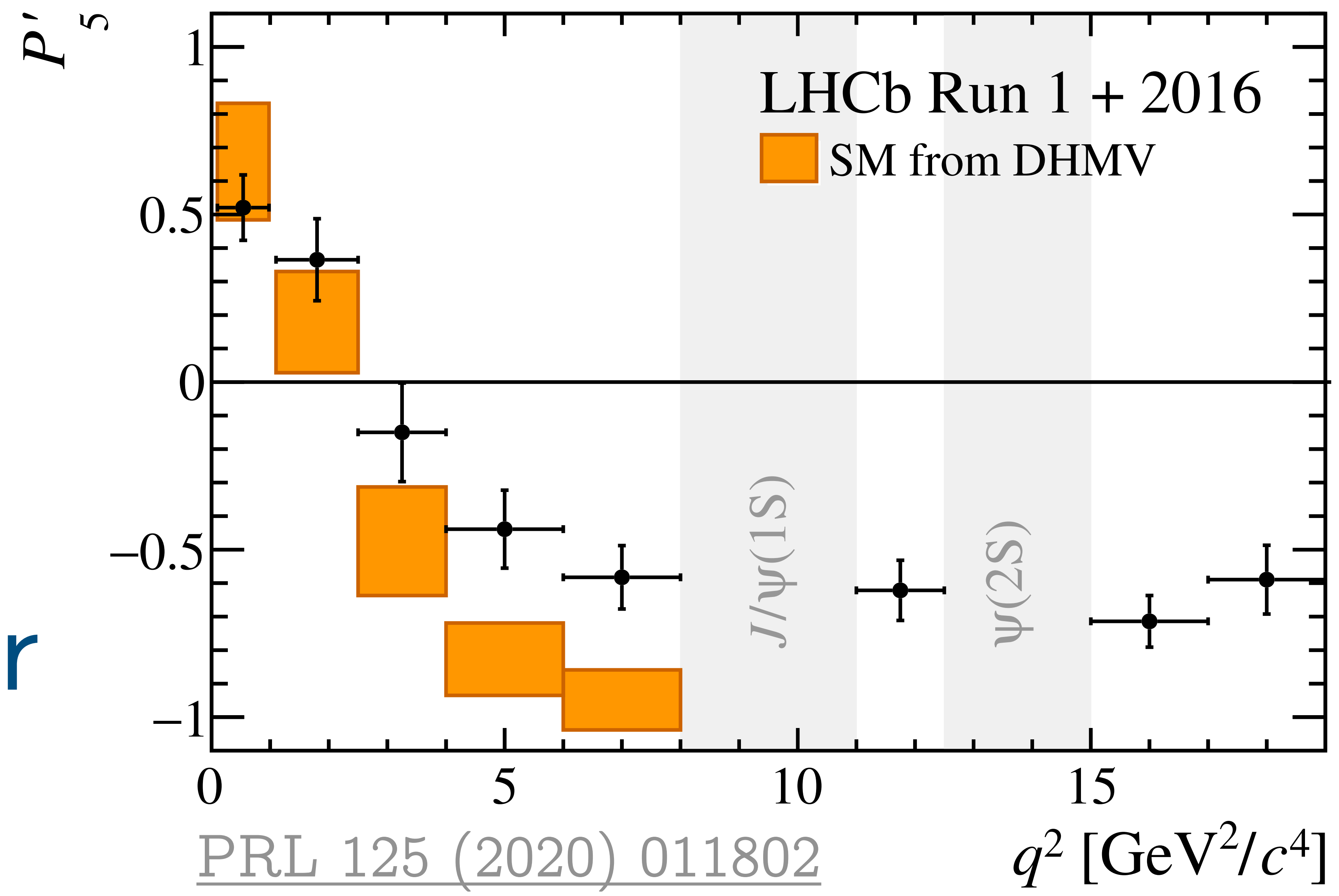

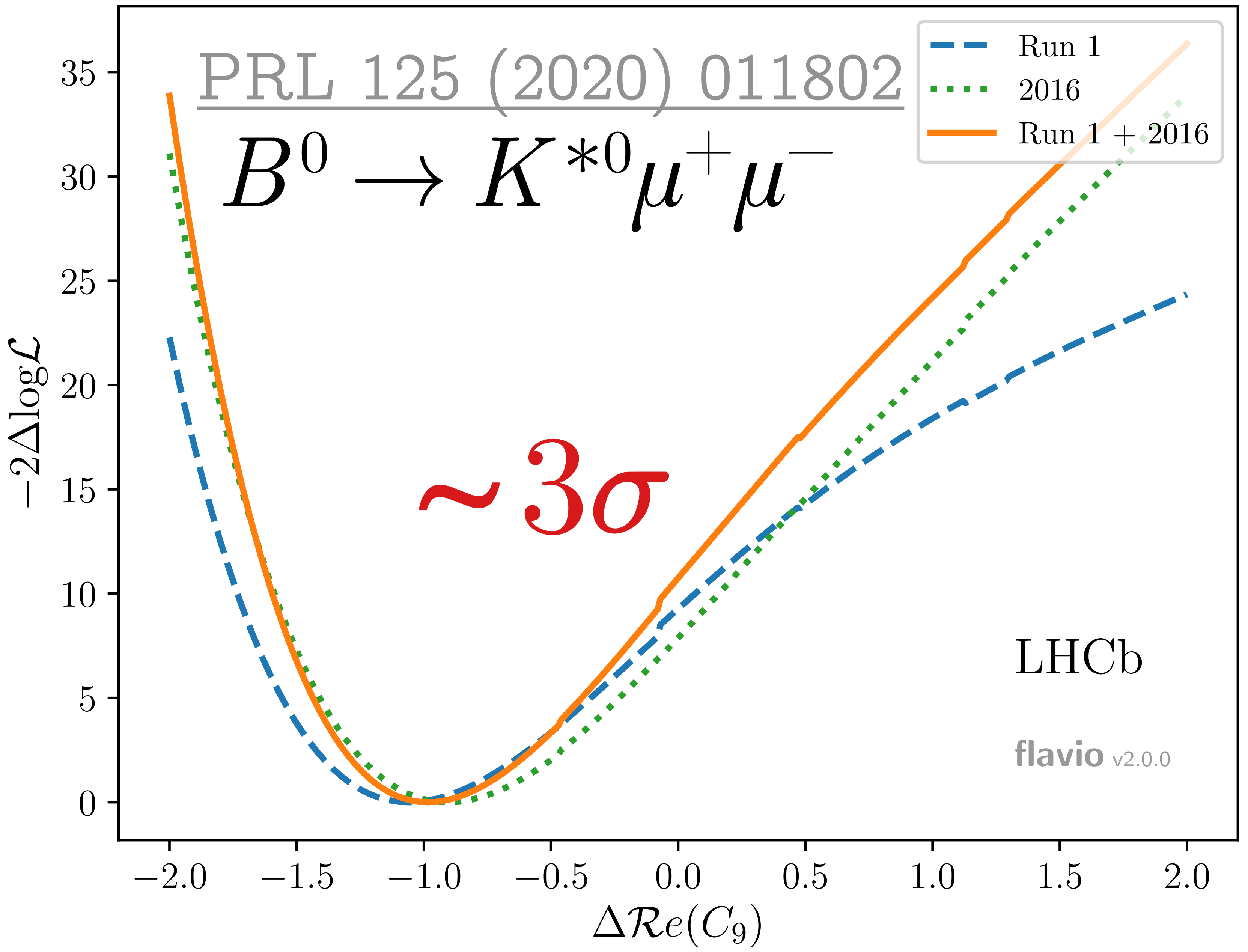

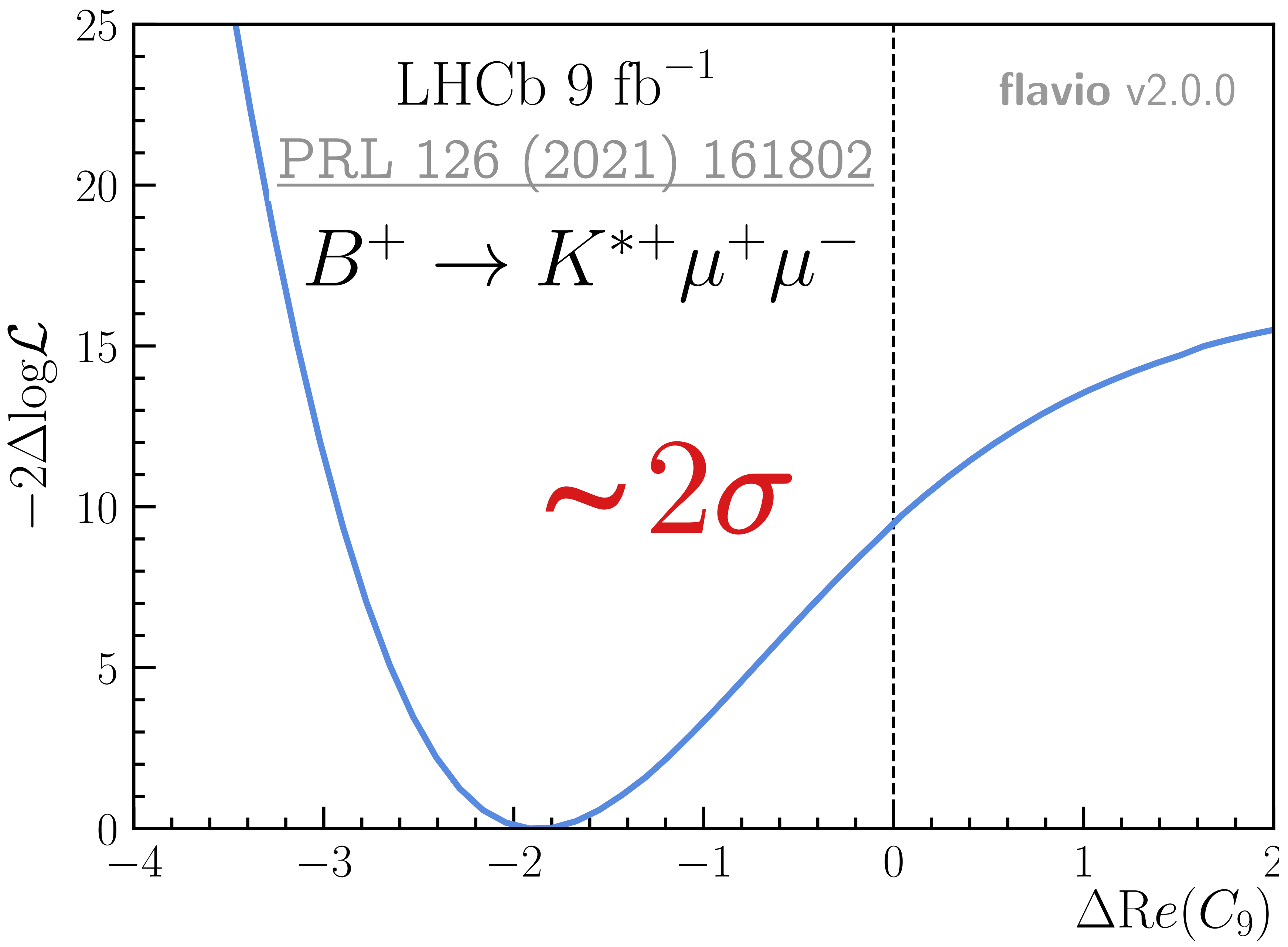

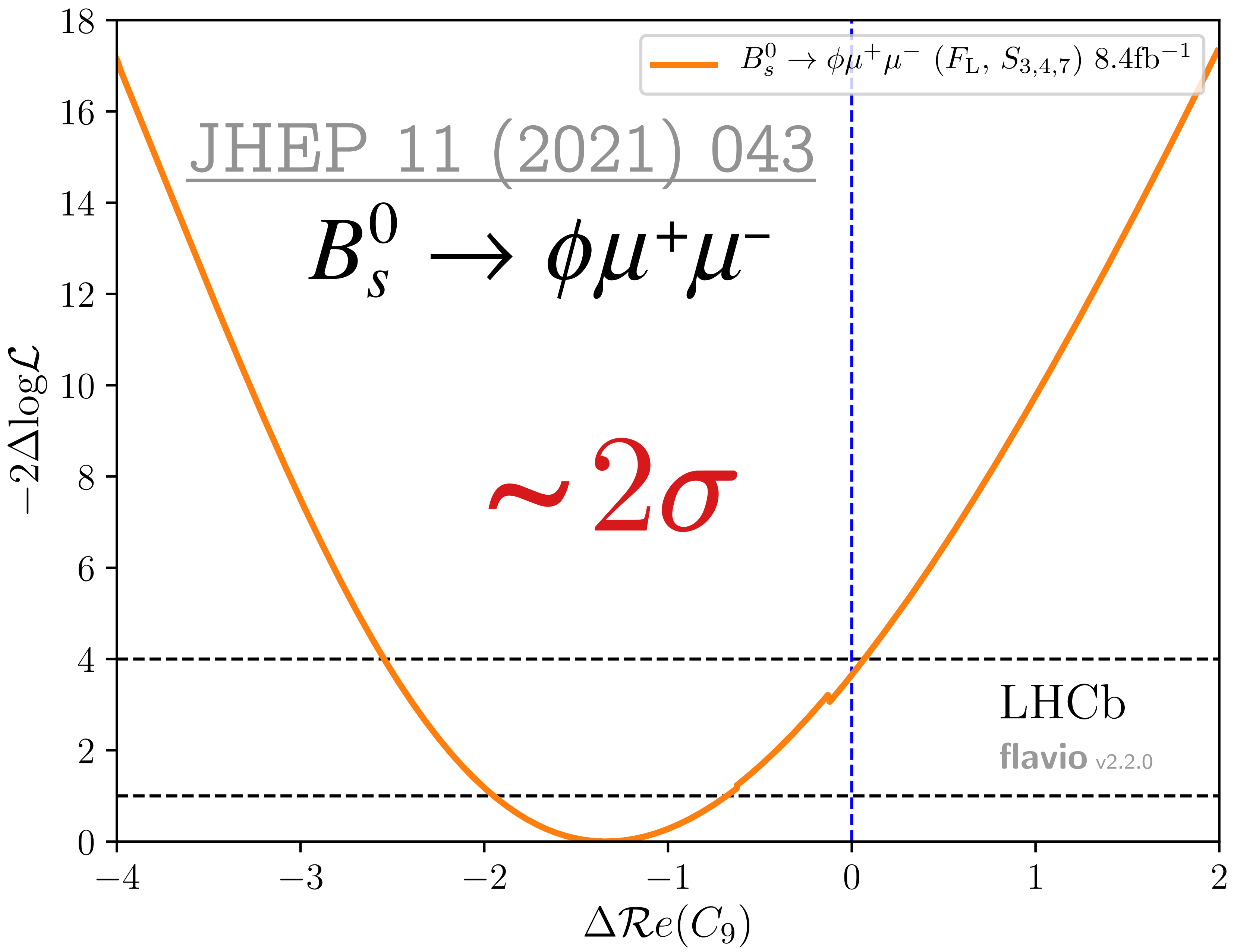

… prefer shifts of effective couplings.

SM $c\bar{c}$ loop

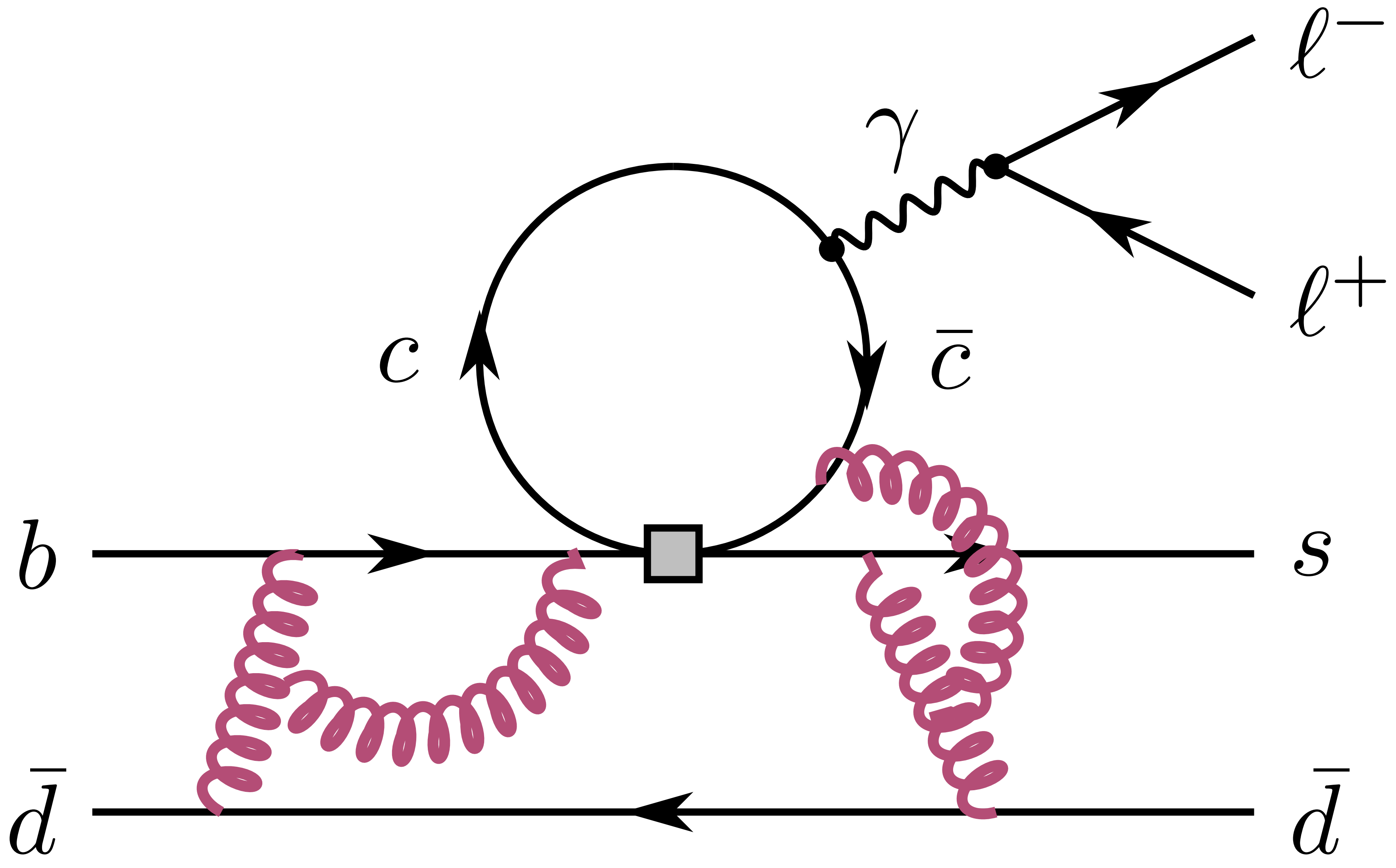

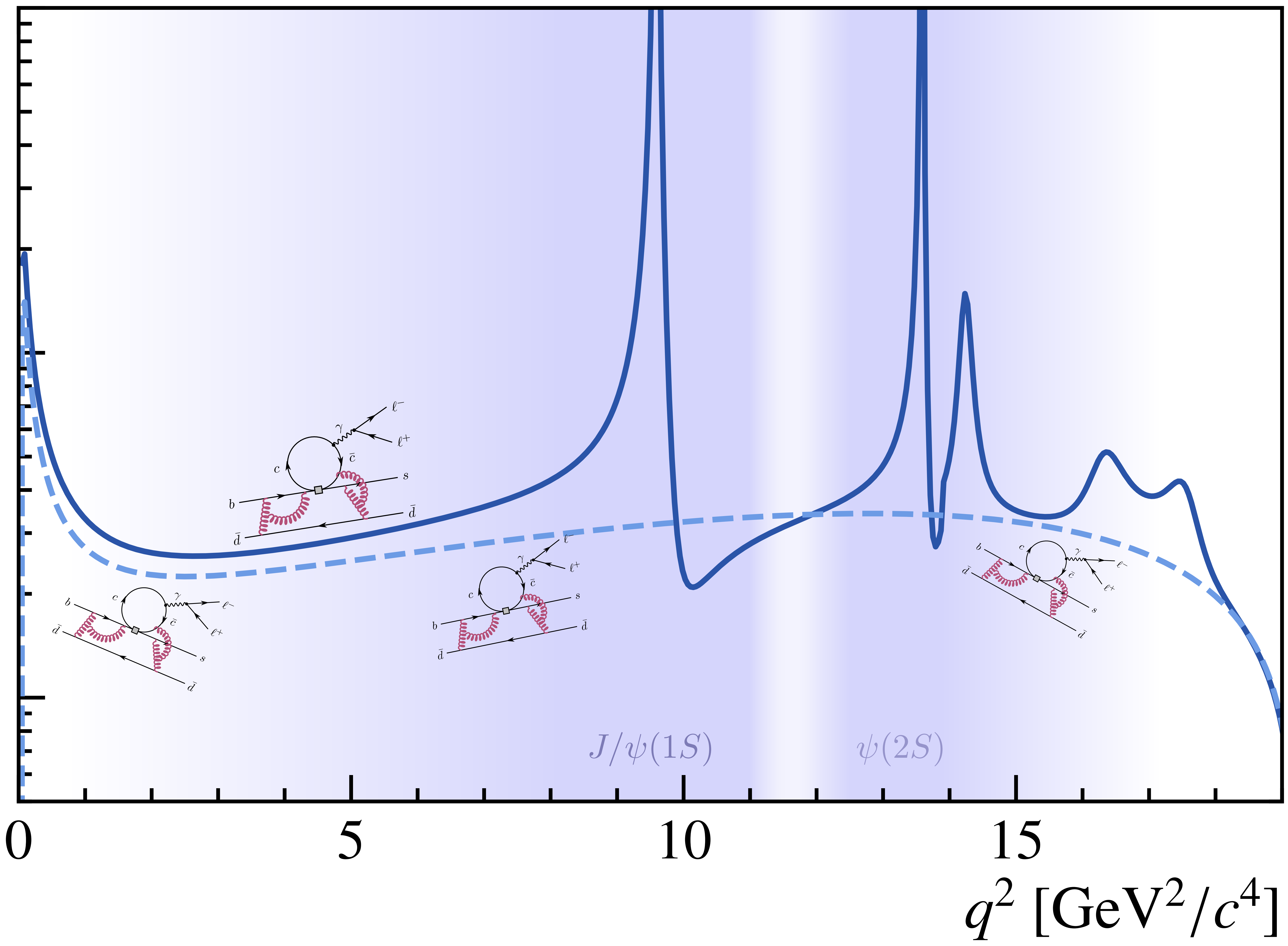

SM $c\bar{c}$ loop

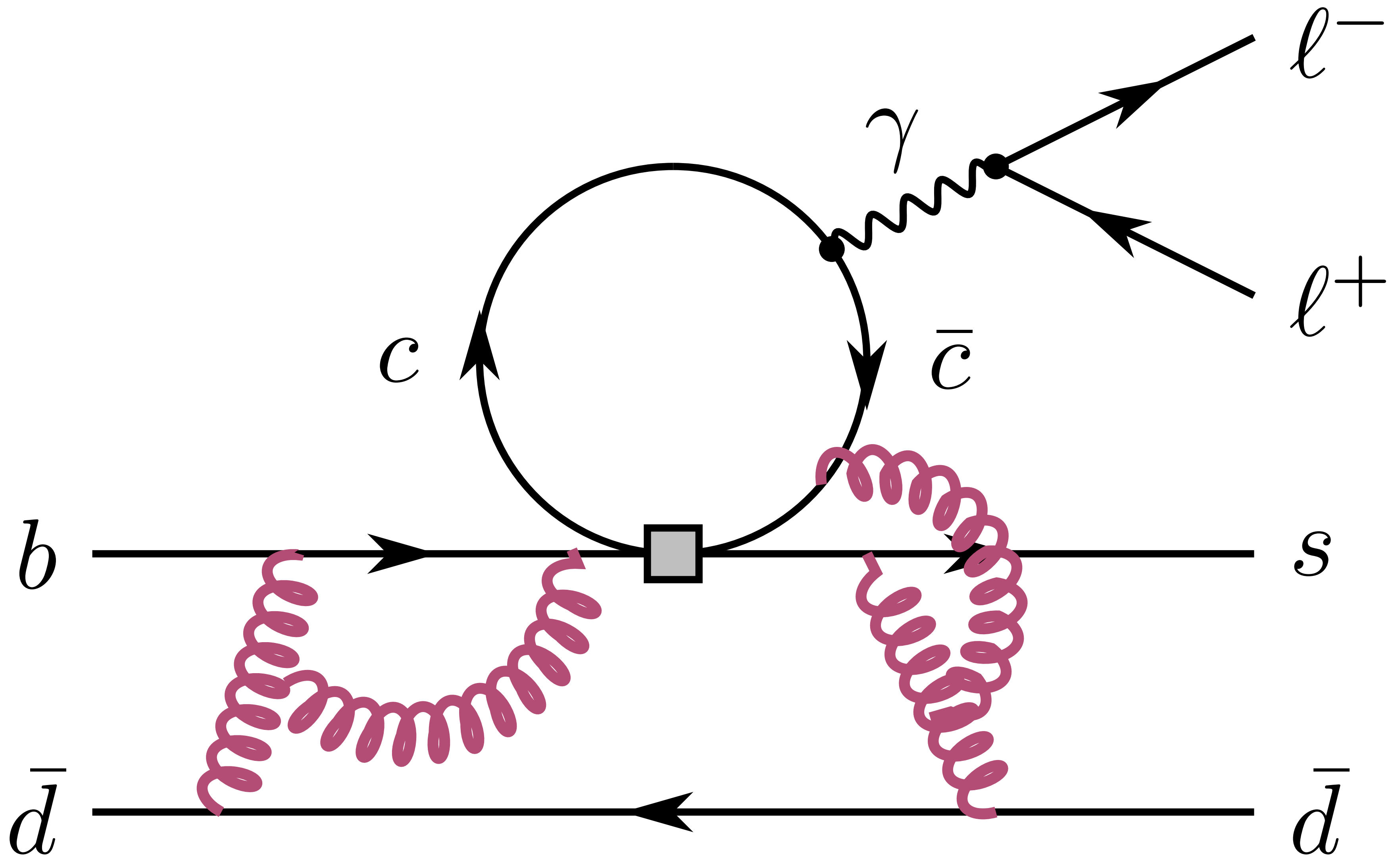

Get this from data

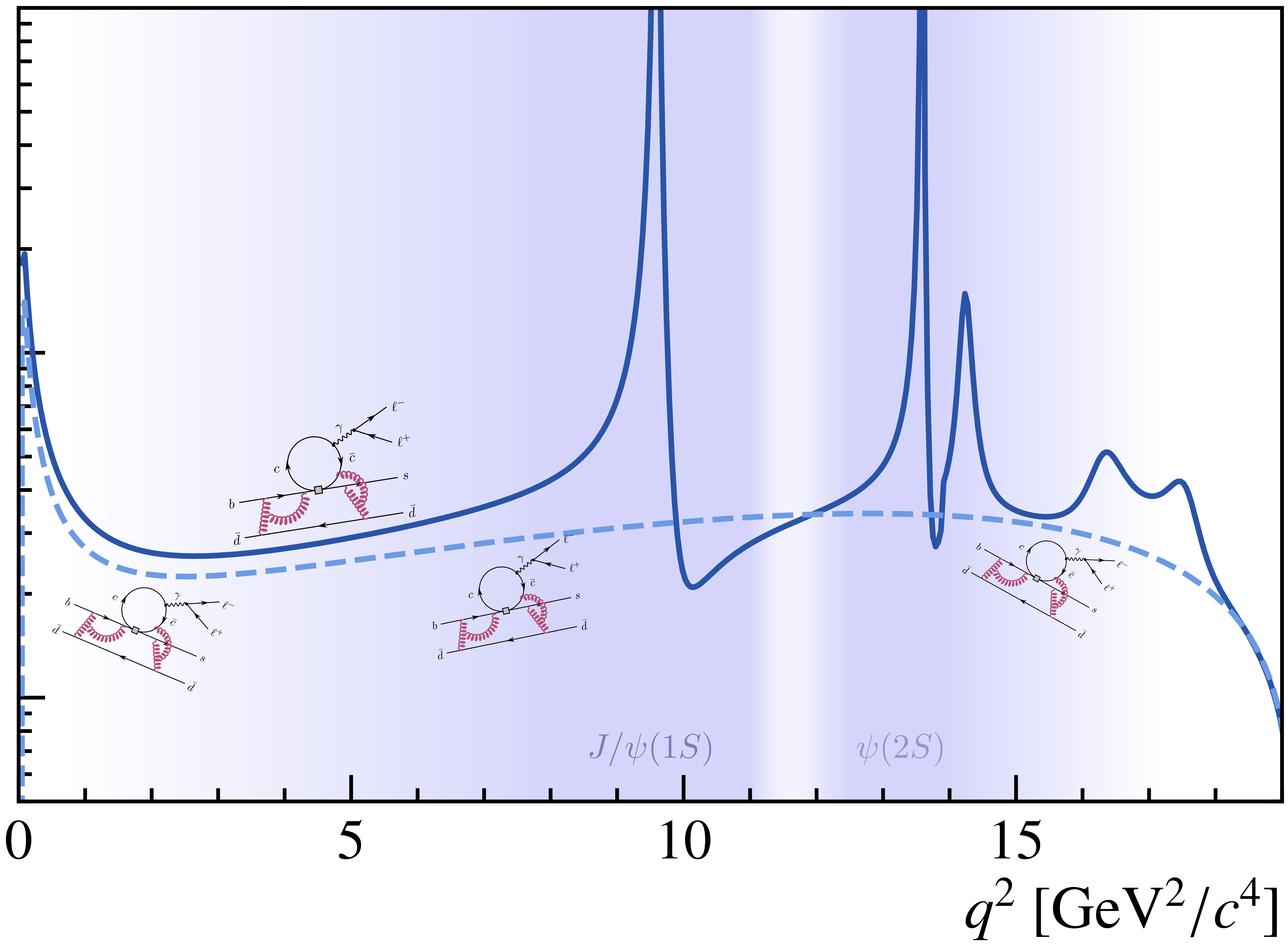

Unbinned amplitude analysis

Slide from A. Mauri CKM '23

- Perform q^2 unbinned amplitude analysis
  - model *local* vs *non-local* contributions

non-local hadronic matrix elements
"charm-loop"

$$\mathcal{A}_\lambda^{L,R} = \mathcal{N}_\lambda \left\{ \left[(\mathcal{C}_9 \pm \mathcal{C}_9') \mp (\mathcal{C}_{10} \pm \mathcal{C}_{10}') \right] \mathcal{F}_\lambda(q^2) + \frac{2 m_b M_B}{q^2} \left[(\mathcal{C}_7 \pm \mathcal{C}_7') \mathcal{F}_\lambda^T(q^2) - 16\pi^2 \frac{M_B}{m_b} \mathcal{H}_\lambda(q^2) \right] \right\}$$

$\lambda = \perp, \parallel, 0$

Wilson coeff.

Form Factors

polynomial expansion

JHEP 09 (2022) 133

$$\mathcal{H}_\lambda(z) = \frac{1 - z z_{J/\psi}^*}{z - z_{J/\psi}} \frac{1 - z z_{\psi(2S)}^*}{z - z_{\psi(2S)}} \times \ldots \times \sum_n \alpha_{\lambda,n} z^n$$

- **Fit 5-D differential decay rate!**

  ↳ $q^2, m_{K\pi}^2, \cos\theta_\ell, \theta_K, \phi$

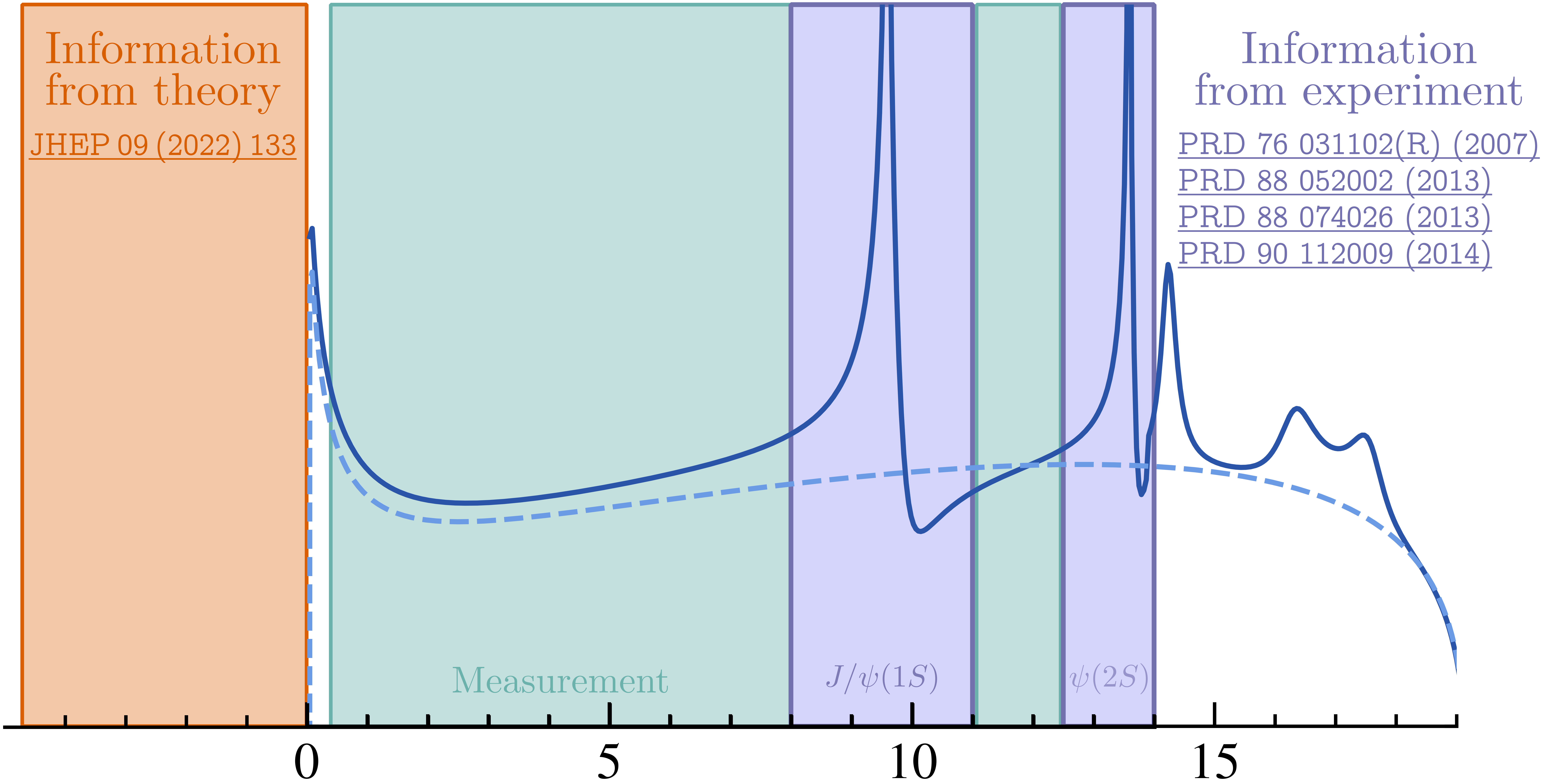

Analysis performed with and without $q^2 < 0$ theory prior

Results: charm-loop matrix elements

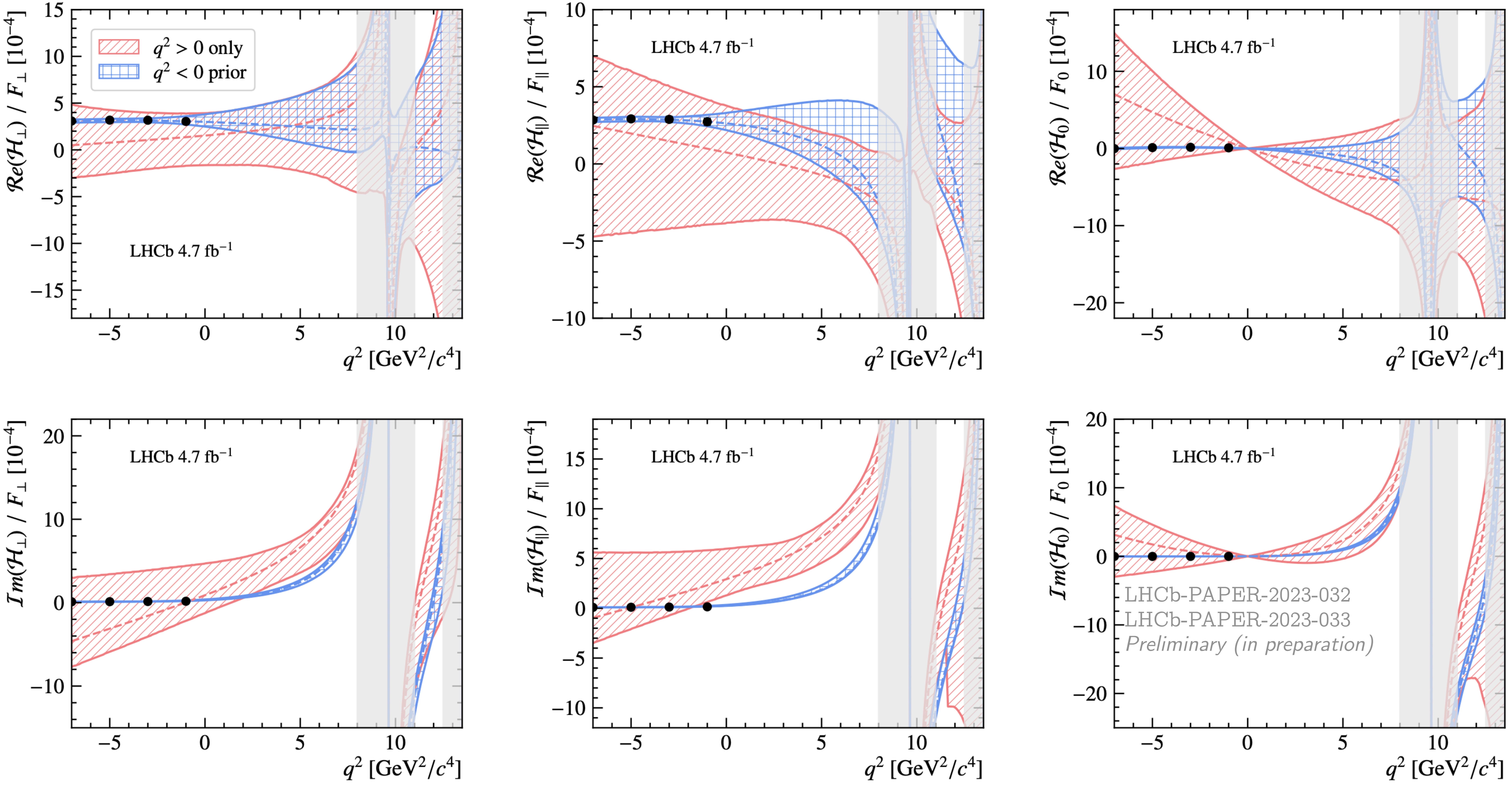

Fit results compatible, some discrepancy in the imaginary parts

Results: form-factors

Good overall agreement with theory, mild preference for lower $F_{\perp,\parallel}/F_0$

Results: $\mathrm{d}\mathcal{B}/\mathrm{d}q^2$ and P_5'

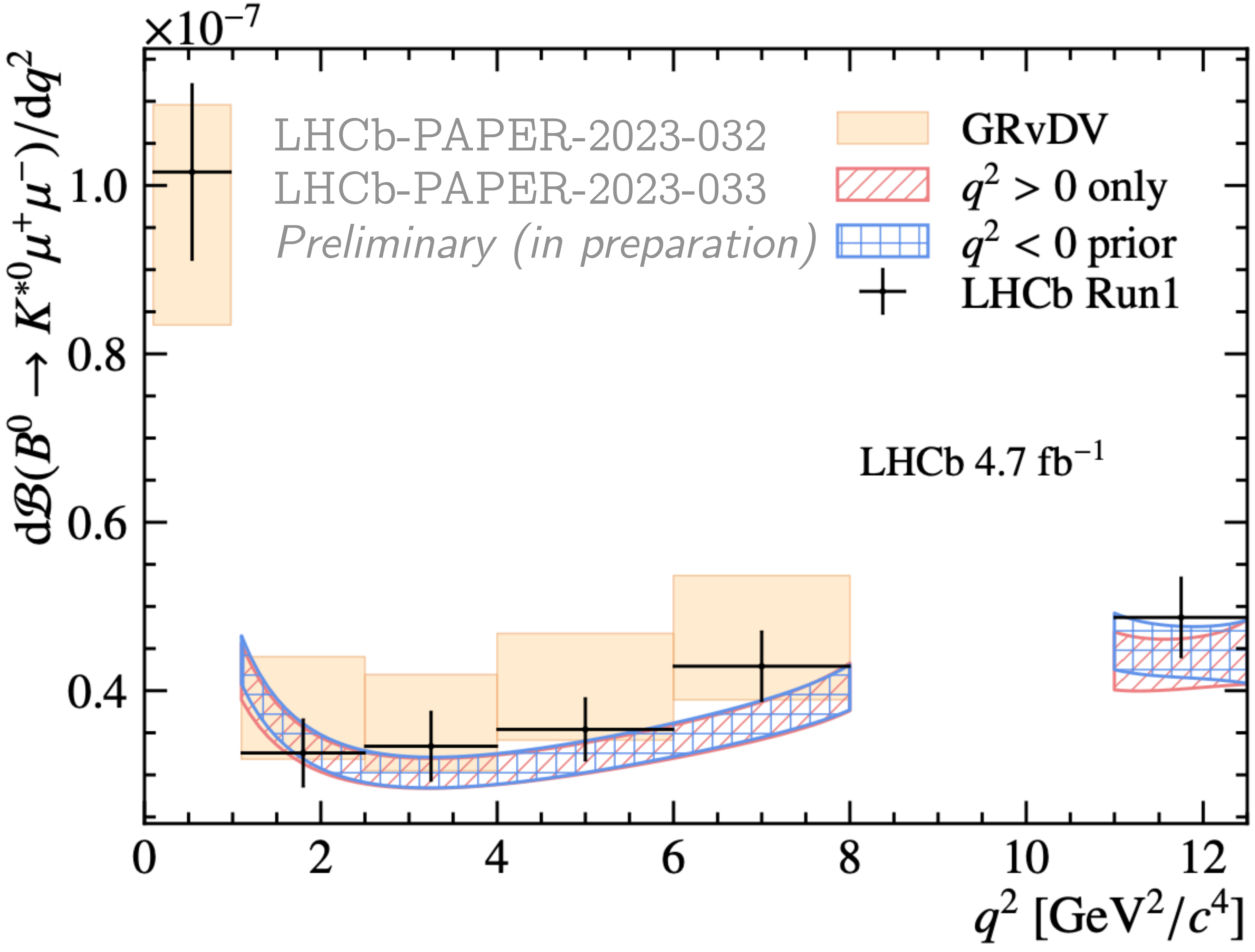

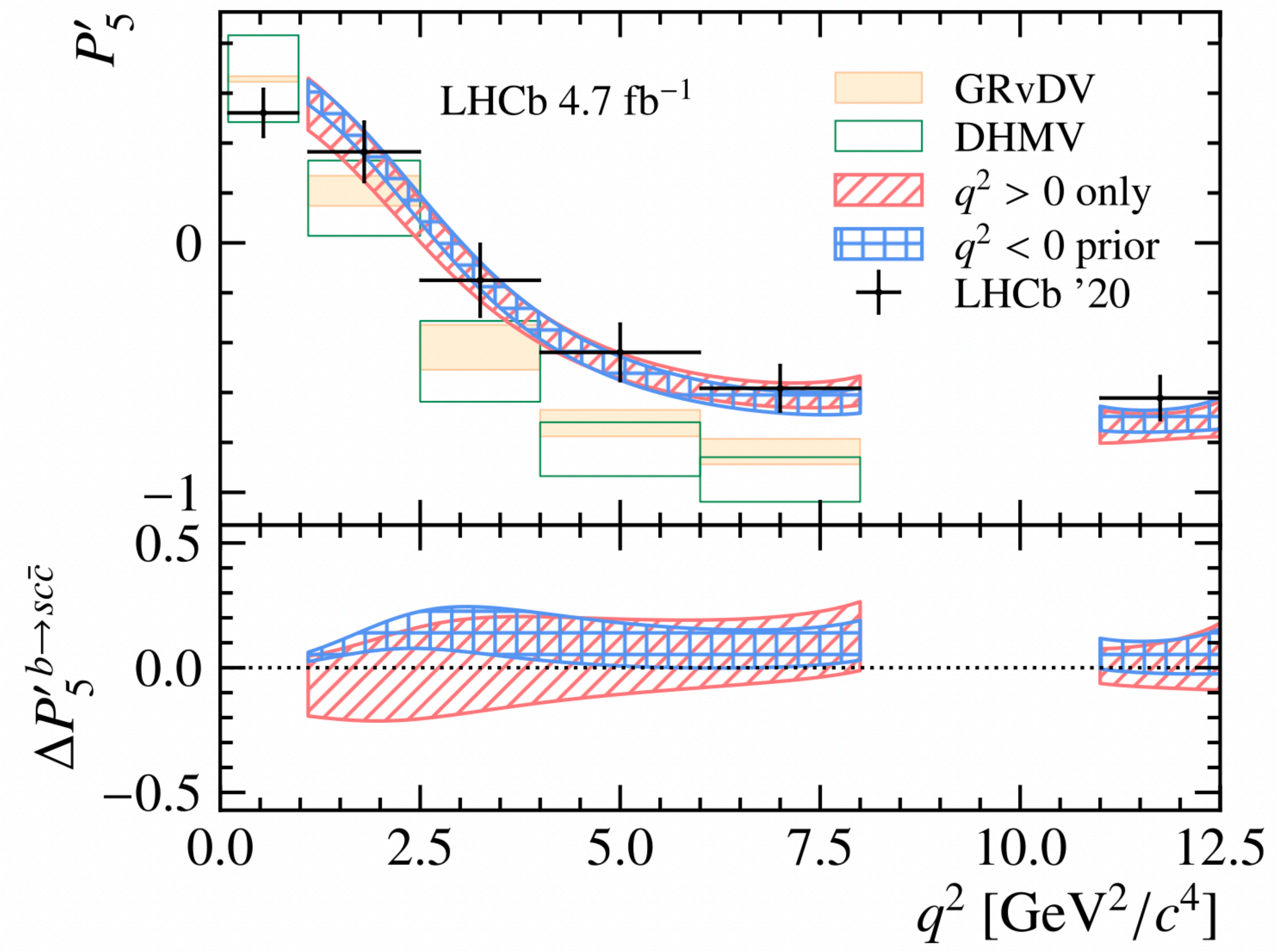

Updated normalisation inputs
⇒ lower BR *cf.* Run 1

Great agreement w/ binned result
Impact of $c\bar{c}$ up to 20%

Results: Wilson coefficients

	$q^2 > 0$ only	
	Fit result	deviation from SM
$\mathcal{C}_9$	$-0.93^{+0.53}_{-0.57}$	$1.9\ \sigma$
$\mathcal{C}_{10}$	$0.48^{+0.29}_{-0.31}$	$1.5\ \sigma$
$\mathcal{C}'_9$	$0.48^{+0.49}_{-0.55}$	$0.9\ \sigma$
$\mathcal{C}'_{10}$	$0.38^{+0.28}_{-0.25}$	$1.5\ \sigma$
	$q^2 < 0$ prior	
$\mathcal{C}_9$	$-0.68^{+0.33}_{-0.46}$	$1.8\ \sigma$
$\mathcal{C}_{10}$	$0.24^{+0.27}_{-0.28}$	$0.9\ \sigma$
$\mathcal{C}'_9$	$0.26^{+0.40}_{-0.48}$	$0.5\ \sigma$
$\mathcal{C}'_{10}$	$0.27^{+0.25}_{-0.27}$	$1.0\ \sigma$

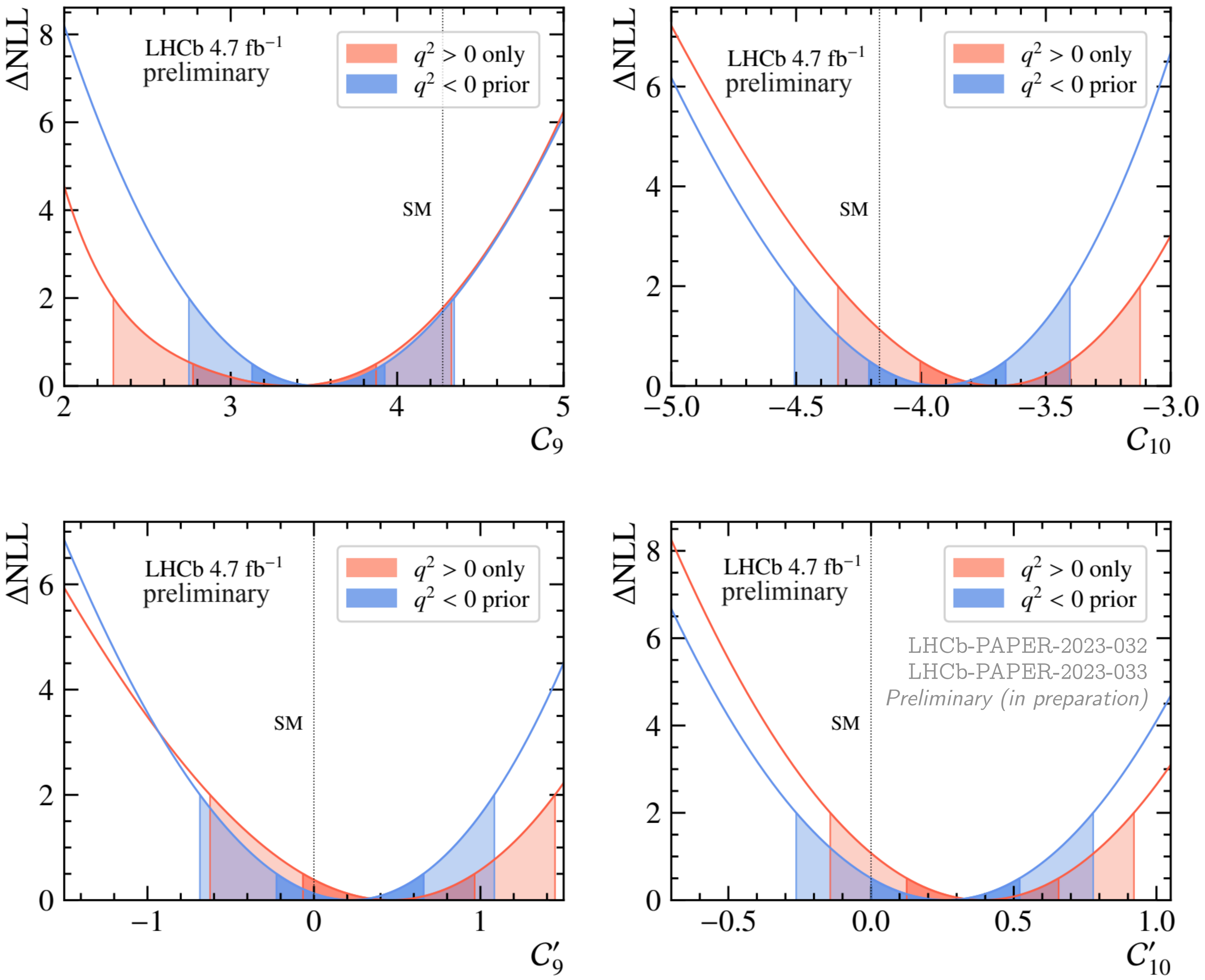

Data — SM tension $\sim 1.9\,\sigma$ in C_9, up to $1.5\,\sigma$ in C_{10}

Results: Wilson coefficients

Data — SM tension $\sim 1.9\,\sigma$ in C_9, up to $1.5\,\sigma$ in C_{10}

Combined tension $\sim 1.4\,\sigma$

Summary of $b \to s\ell^+\ell^-$ LFU & anomalies at LHCb

LFU-sensitive R_{H_s} ratios

- compatible with SM within 5%
- e^+e^- challenging but well understood
- experimental bottleneck: statistics

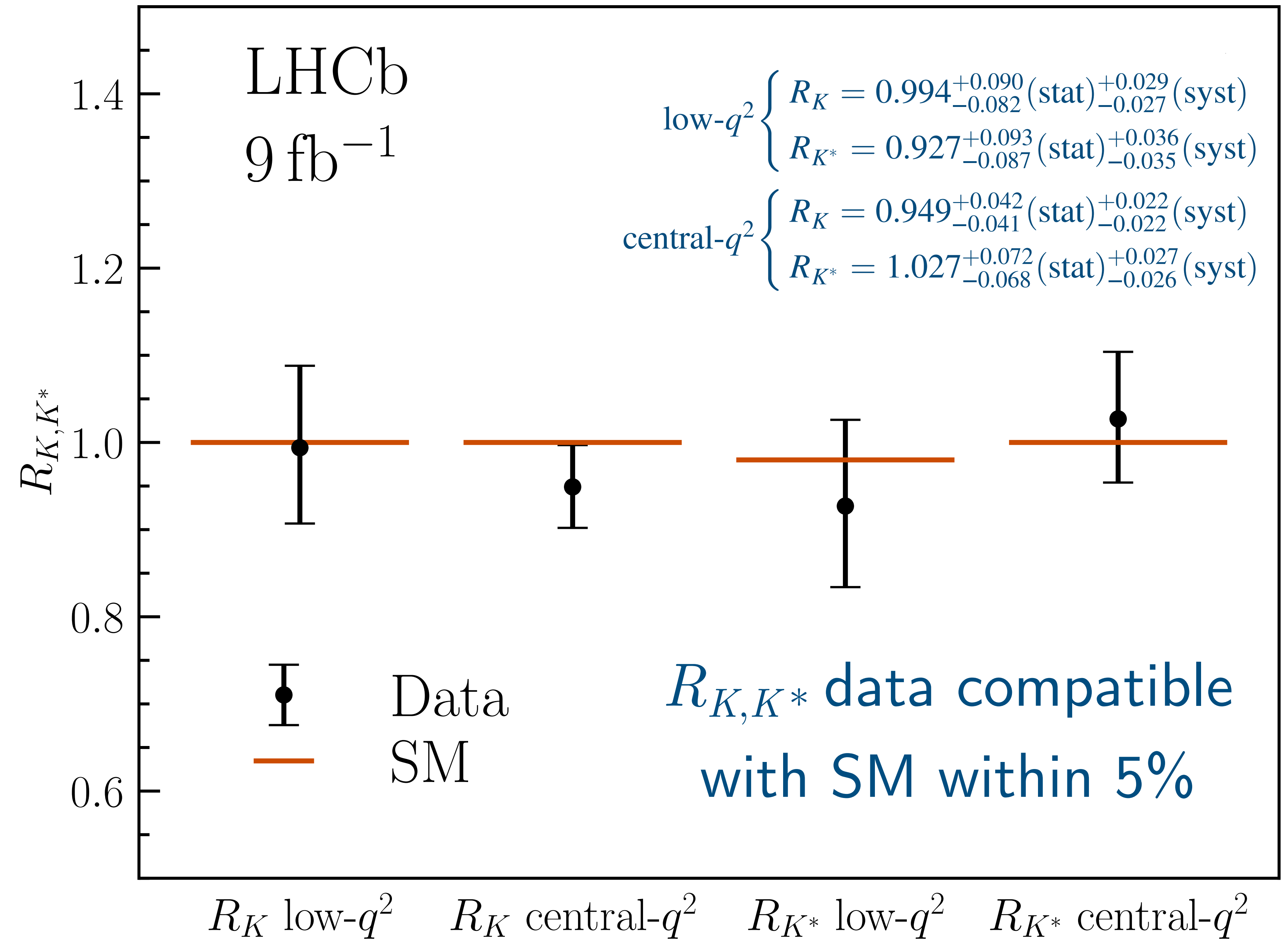

BFs and angular obs.

- systematic deviations from SM
- not just non-local contributions
- theory feedback crucial for progress

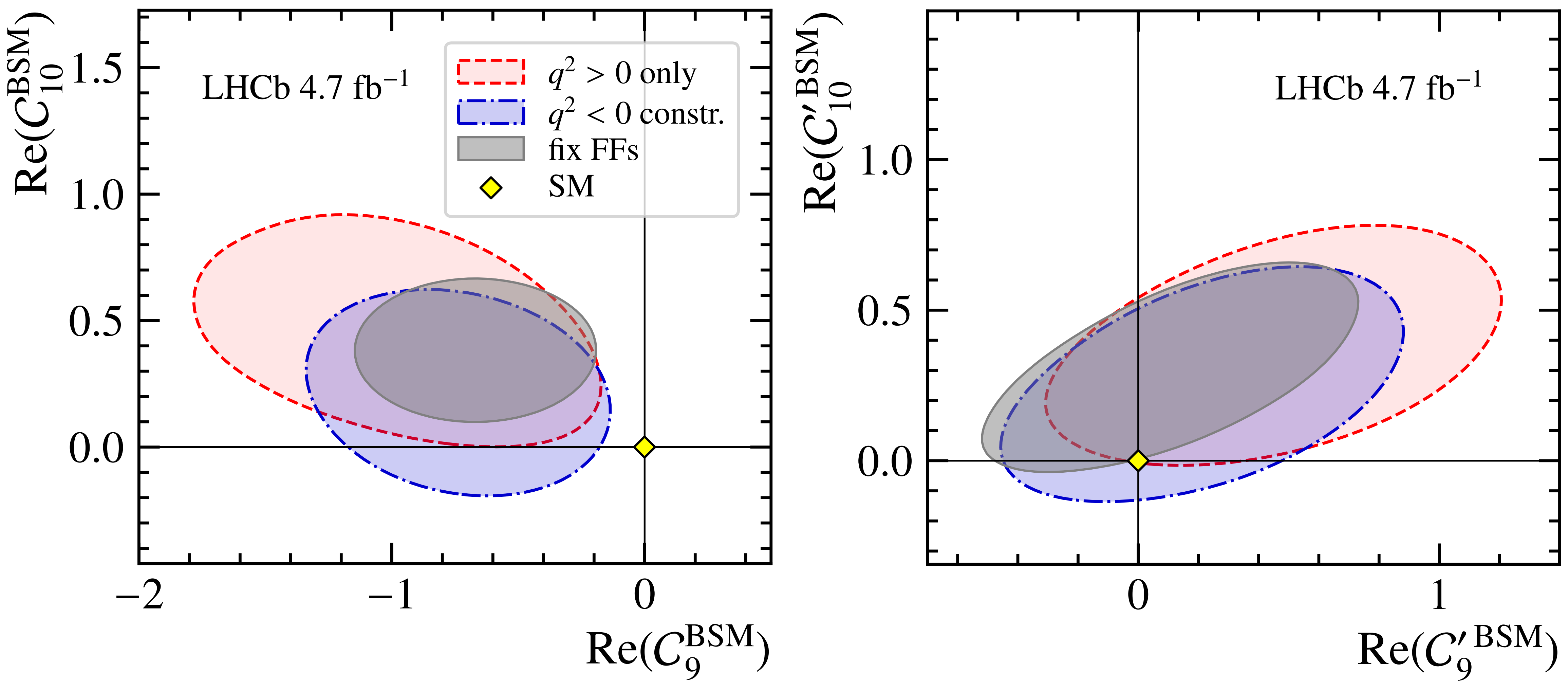

Summary of $b \to s\ell^+\ell^-$ LFU & anomalies at LHCb

We've come a long way,
and there's still plenty to do.

BACKUP

Theory information

Value of charm-loop at $q^2 < 0$

▷ reliable for $q^2 \ll 4m_c^2$

JHEP 09 (2022) 133

Experimental measurements

Branching ratio, polarization fraction and phase difference from $B^0 \to \psi_n K^{*0}$

PRD 76 031102(R) (2007)
PRD 88 052002 (2013)
PRD 88 074026 (2013)
PRD 90 112009 (2014)

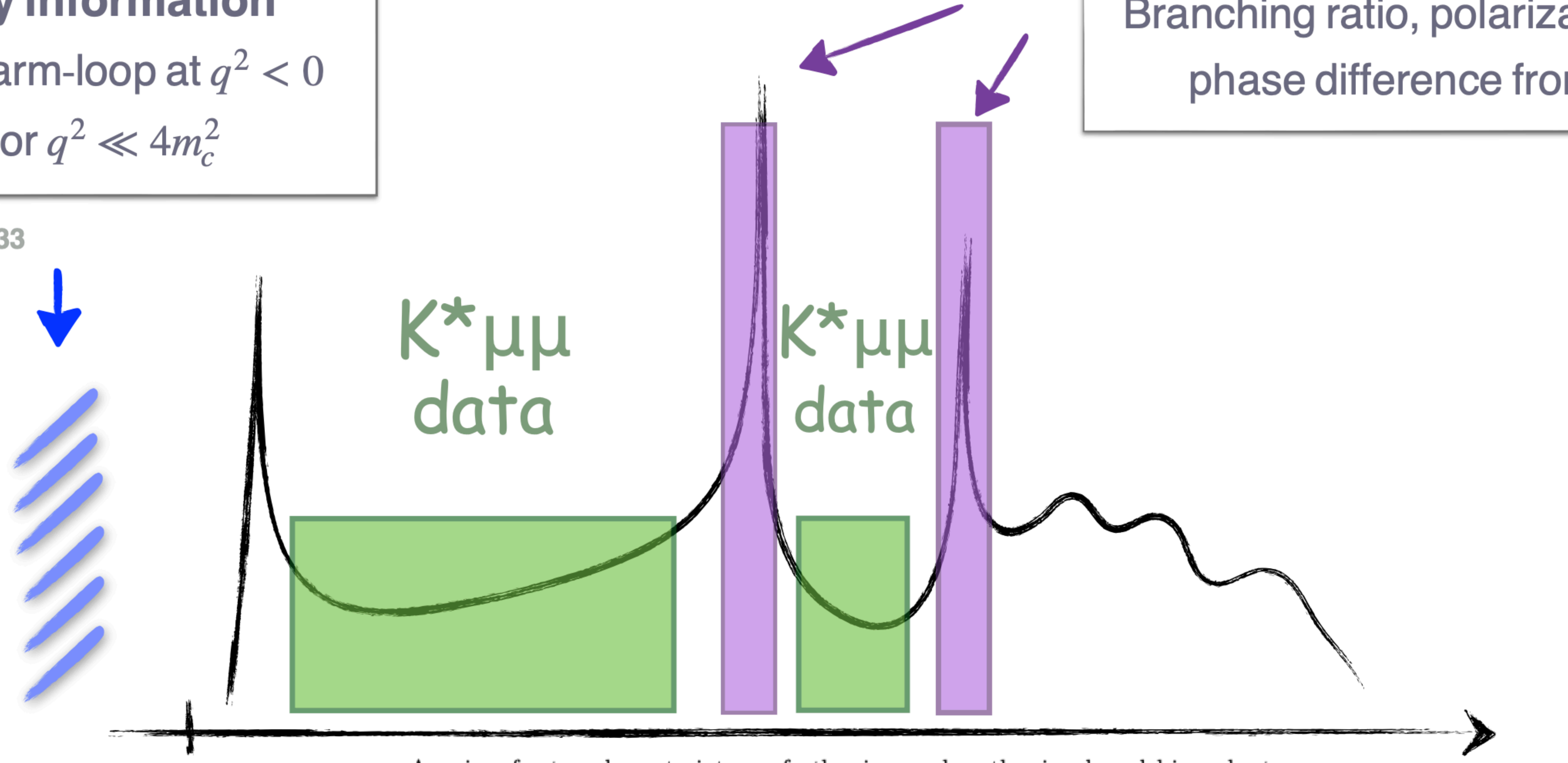

A series of external constraints are further imposed on the signal model in order to ensure the stability of the amplitude fit in a similar fashion to Refs. [36, 37]: the values of the CKM elements that enter in $\mathcal{N}$ are constrained to the values obtained from the SM fit of the Unitarity triangle [58]; the local FFs for the $B^0 \to K^{*0}$ transition are parametrised by fitting the combined information from Refs. [23, 36] and [30]; and the form factors for the S-wave amplitudes are constrained from Ref. [28] but have their uncertainties inflated by a factor of three to account for differences between $B^0 \to K^+\pi^-$ and $B^0 \to K^0$ transitions. The magnitudes and phases of the resonant amplitudes for the $B^0 \to \psi_n K^{*0}$ decays are instrumental to constrain non-local FFs at the J/ψ and $\psi(2S)$ resonance poles. These are taken from measurements by both LHCb and B-factory experiments [57, 59–62]. Finally, the SM predictions for the real and imaginary parts of the ratio $\mathcal{H}_\lambda/\mathcal{F}_\lambda$ in the negative q^2 region are taken from Ref. [34, 36] and are used as constraints in the fit.

$$
\begin{array}{rrclrcl}
\text{Photon penguin} & \mathcal{O}_7 & = & \frac{m_b}{g_e}(\bar{s}\sigma^{\mu\nu}b_R)F_{\mu\nu} & \mathcal{O}_7' & = & \frac{m_b}{g_e}(\bar{s}\sigma^{\mu\nu}b_L)F_{\mu\nu} \\
\text{Vector penguin} & \mathcal{O}_9 & = & (\bar{s}\gamma_\mu b_L)(\bar{\ell}\gamma^\mu\ell) & \mathcal{O}_9' & = & (\bar{s}\gamma_\mu b_R)(\bar{\ell}\gamma^\mu\ell) \\
\text{Axial vector penguin} & \mathcal{O}_{10} & = & (\bar{s}\gamma_\mu b_L)(\bar{\ell}\gamma^\mu\gamma_5\ell) & \mathcal{O}_{10}' & = & (\bar{s}\gamma_\mu b_R)(\bar{\ell}\gamma^\mu\gamma_5\ell) \\
\text{Scalar} & \mathcal{O}_S & = & (\bar{s}b_R)(\bar{\ell}\ell) & \mathcal{O}_S' & = & (\bar{s}b_L)(\bar{\ell}\ell) \\
\text{Pseudoscalar} & \mathcal{O}_P & = & (\bar{s}b_R)(\bar{\ell}\gamma_5\ell) & \mathcal{O}_P' & = & (\bar{s}b_L)(\bar{\ell}\gamma_5\ell)
\end{array}
$$

$$
\begin{aligned}
\mathcal{F}_\perp &\mapsto \frac{\sqrt{2\lambda(M_B^2, q^2, k^2)}}{M_B(M_B + M_{K^{*0}})} V\,, \\
\mathcal{F}_\parallel &\mapsto \frac{\sqrt{2}(M_B + M_{K^{*0}})}{M_B} A_1\,, \\
\mathcal{F}_0 &\mapsto \frac{(M_B^2 - q^2 - M_{K^{*0}}^2)(M_B + M_{K^{*0}})^2 A_1 - \lambda(M_B^2, q^2, k^2) A_2}{2 M_{K^{*0}} M_B^2 (M_B + M_{K^{*0}})}\,, \\
\mathcal{F}_\perp^T &\mapsto \frac{\sqrt{2\lambda(M_B^2, q^2, k^2)}}{M_B^2} T_1\,, \\
\mathcal{F}_\parallel^T &\mapsto \frac{\sqrt{2}(M_B^2 - M_{K^{*0}}^2)}{M_B^2} T_2\,, \\
\mathcal{F}_0^T &\mapsto \frac{q^2(M_B^2 + 3M_{K^{*0}}^2 - q^2)}{2 M_B^3 M_{K^{*0}}} T_2 - \frac{q^2 \lambda(M_B^2, q^2, k^2)}{2 M_B^3 M_{K^{*0}} (M_B^2 - M_{K^{*0}}^2)} T_3\,, \\
\mathcal{F}_t &\mapsto \frac{\sqrt{\lambda(M_B^2, q^2, k^2)}}{M_B \sqrt{q^2}} A_0\,.
\end{aligned}
$$

$$
\begin{aligned}
\frac{\mathrm{d}^4\Gamma[B^0 \to K^{*0}\mu^+\mu^-]}{\mathrm{d}q^2\,\mathrm{d}\vec{\Omega}} &= \frac{9}{32\pi}\sum_i I_i(q^2) f_i(\vec{\Omega}) \\
&= \frac{9}{32\pi}\Big[I_{1s}\sin^2\theta_K + I_{1c}\cos^2\theta_K + \\
&\quad I_{2s}\sin^2\theta_K\cos 2\theta_\ell + I_{2c}\cos^2\theta_K\cos 2\theta_\ell + \\
&\quad I_3\sin^2\theta_K\sin^2\theta_\ell\cos 2\phi + I_4\sin 2\theta_K\sin 2\theta_\ell\cos\phi + \\
&\quad I_5\sin 2\theta_K\sin\theta_\ell\cos\phi + I_6\sin^2\theta_K\cos\theta_\ell + \\
&\quad I_7\sin 2\theta_K\sin\theta_\ell\sin\phi + I_8\sin 2\theta_K\sin 2\theta_\ell\sin\phi + \\
&\quad I_9\sin^2\theta_K\sin^2\theta_\ell\sin 2\phi \Big],
\end{aligned}
$$

Ignoring scalar and tensor operators, the P-wave angular coefficients entering in Eq. 1 are

$$
\begin{aligned}
I_{1s} &= \frac{2+\beta_l^2}{4}\Big[|\mathcal{A}_\perp^L|^2 + |\mathcal{A}_\parallel^L|^2 + (L\to R)\Big] + \frac{4m_l^2}{q^2}\mathcal{R}e\Big(\mathcal{A}_\perp^L\mathcal{A}_\perp^{R*} + \mathcal{A}_\parallel^L\mathcal{A}_\parallel^{R*}\Big), \\
I_{1c} &= \Big[|\mathcal{A}_0^L|^2 + |\mathcal{A}_0^R|^2\Big] + \frac{4m_l^2}{q^2}\Big[|\mathcal{A}_t|^2 + 2\,\mathcal{R}e(\mathcal{A}_0^L\mathcal{A}_0^{R*})\Big], \\
I_{2s} &= \frac{\beta_l^2}{4}\Big[|\mathcal{A}_\perp^L|^2 + |\mathcal{A}_\parallel^L|^2 + (L\to R)\Big], \\
I_{2c} &= -\beta_l^2\Big[|\mathcal{A}_0^L|^2 + |\mathcal{A}_0^R|^2\Big], \\
I_3 &= \frac{\beta_l^2}{2}\Big[|\mathcal{A}_\perp^L|^2 - |\mathcal{A}_\parallel^L|^2 + (L\to R)\Big], \\
I_4 &= -1\times\frac{\beta_l^2}{\sqrt{2}}\mathcal{R}e\Big[\mathcal{A}_0^L\mathcal{A}_\parallel^{L*} + (L\to R)\Big], \\
I_5 &= \sqrt{2}\beta_l\,\mathcal{R}e\Big[\mathcal{A}_0^L\mathcal{A}_\perp^{L*} - (L\to R)\Big], \\
I_{6s} &= -1\times 2\beta_l\,\mathcal{R}e\Big[\mathcal{A}_\parallel^L\mathcal{A}_\perp^{L*} - (L\to R)\Big], \\
I_7 &= -1\times\sqrt{2}\beta_l\,\mathcal{I}m\Big[\mathcal{A}_0^L\mathcal{A}_\parallel^{L*} - (L\to R)\Big], \\
I_8 &= \frac{\beta_l^2}{\sqrt{2}}\mathcal{I}m\Big[\mathcal{A}_0^L\mathcal{A}_\perp^{L*} + (L\to R)\Big], \\
I_9 &= -1\times\beta_l^2\,\mathcal{I}m\Big[\mathcal{A}_\perp^L\mathcal{A}_\parallel^{L*} + (L\to R)\Big],
\end{aligned}
\tag{15}
$$

where the sign -1 in front of $I_{4,6s,7,9}$ is due to the adoption of the LHCb angular notation as opposite to the theory convention [75] and $\beta_l = \sqrt{1-4m_l^2/q^2}$, with m_l the mass of the

$$
\begin{aligned}
\frac{32\pi}{9}\frac{\mathrm{d}^5\Gamma}{\mathrm{d}q^2\,\mathrm{d}k^2\,\mathrm{d}\vec{\Omega}} &= \frac{32\pi}{9}\frac{\mathrm{d}^5\Gamma}{\mathrm{d}q^2\,\mathrm{d}k^2\,\mathrm{d}\vec{\Omega}}\Big|_{\mathrm{P-wave}} \\
&+ \Big(I_{1c}^S + I_{2c}^S\cos 2\theta_l\Big) \\
&+ \Big(\tilde{I}_{1c} + \tilde{I}_{2c}\cos 2\theta_l\Big)\cos\theta_K \\
&+ \Big(\tilde{I}_4\sin 2\theta_l + \tilde{I}_5\sin\theta_l\Big)\sin\theta_K\cos\phi \\
&+ \Big(\tilde{I}_7\sin\theta_l + \tilde{I}_8\sin 2\theta_l\Big)\sin\theta_K\sin\phi
\end{aligned}
$$

lepton. Similarly, the introduction of the S-wave contribution gives origin to the following additional set of angular coefficients

$$
\begin{aligned}
I_{1c}^S &= \frac{1}{3}\Big\{\Big[|\mathcal{A}_{S0}^L|^2 + |\mathcal{A}_{S0}^R|^2\Big] + \frac{4m_l^2}{q^2}\Big[|\mathcal{A}_{St}|^2 + 2\,\mathcal{R}e(\mathcal{A}_{S0}^L\mathcal{A}_{S0}^{R\,*})\Big]\Big\}, \\
I_{2c}^S &= -\frac{1}{3}\beta_l^2\Big[|\mathcal{A}_{S0}^L|^2 + |\mathcal{A}_{S0}^R|^2\Big], \\
\tilde{I}_{1c} &= \frac{2}{\sqrt{3}}\mathcal{R}e\Big[\mathcal{A}_{S0}^L\mathcal{A}_0^{L*} + \mathcal{A}_{S0}^R\mathcal{A}_0^{R*} + \frac{4m_l^2}{q^2}\Big(\mathcal{A}_{S0}^L\mathcal{A}_0^{R*} + \mathcal{A}_0^L\mathcal{A}_{S0}^{R\,*} + \mathcal{A}_{St}\mathcal{A}_t^{\,*}\Big)\Big], \\
\tilde{I}_{2c} &= -\frac{2}{\sqrt{3}}\beta_l^2\,\mathcal{R}e\Big[\mathcal{A}_{S0}^L\mathcal{A}_0^{L*} + \mathcal{A}_{S0}^R\mathcal{A}_0^{R*}\Big], \\
\tilde{I}_4 &= -1\times\sqrt{\frac{2}{3}}\beta_l^2\,\mathcal{R}e\Big[\mathcal{A}_{S0}^L\mathcal{A}_\parallel^{L*} + (L\to R)\Big], \\
\tilde{I}_5 &= \sqrt{\frac{8}{3}}\beta_l^2\,\mathcal{R}e\Big[\mathcal{A}_{S0}^L\mathcal{A}_\perp^{L*} - (L\to R)\Big], \\
\tilde{I}_7 &= -1\times\sqrt{\frac{8}{3}}\beta_l^2\,\mathcal{I}m\Big[\mathcal{A}_{S0}^L\mathcal{A}_\parallel^{L*} - (L\to R)\Big], \\
\tilde{I}_8 &= \sqrt{\frac{2}{3}}\beta_l^2\,\mathcal{I}m\Big[\mathcal{A}_{S0}^L\mathcal{A}_\perp^{L*} + (L\to R)\Big],
\end{aligned}
\tag{16}
$$

where the first two are pure S-wave contributions while the ones denoted $\tilde{I}_i$ raise from interference terms. As above, the -1 in front of $\tilde{I}_{4,7}$ results from the transformation from the theory to the LHCb angular convention.

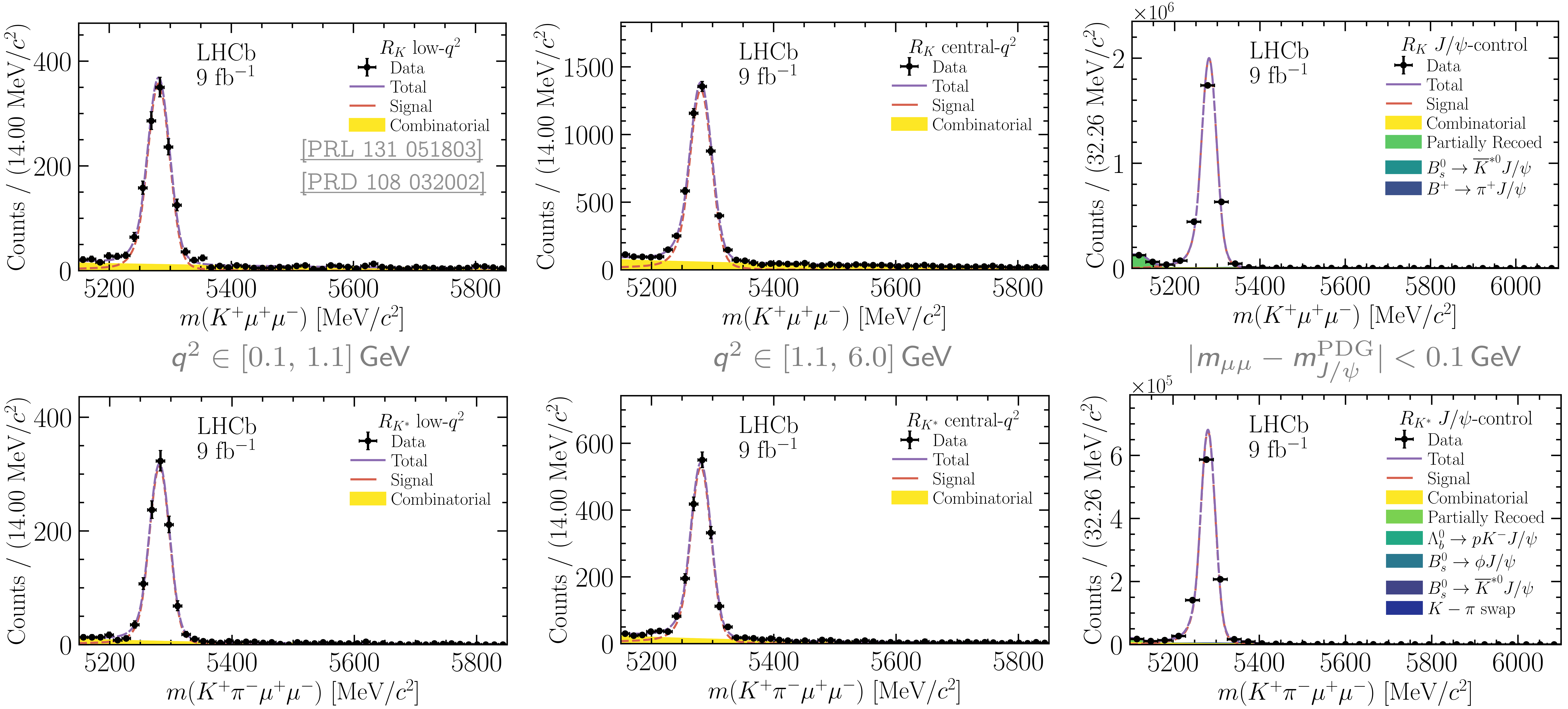

Muons at LHCb have well-defined, very clean peaks.

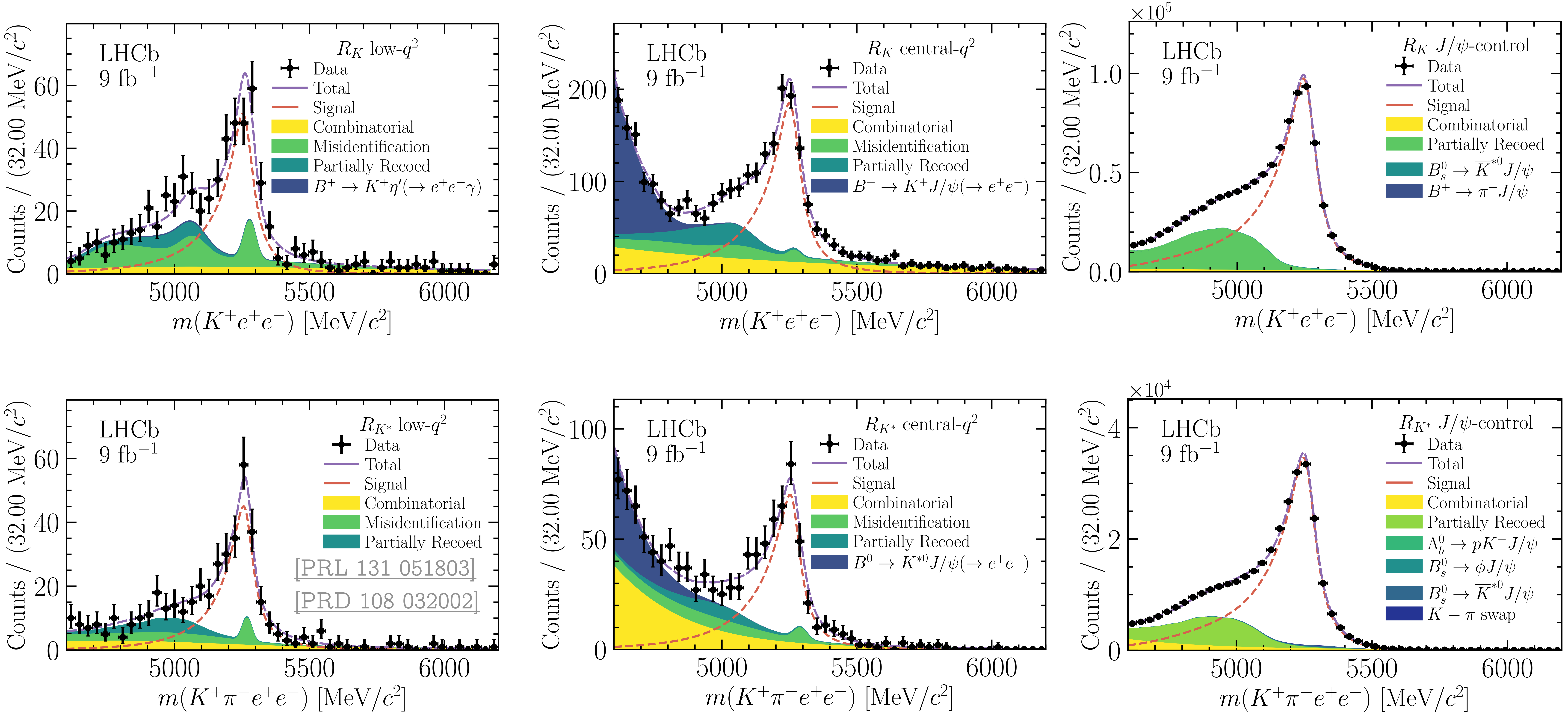

Electrons at LHCb have diminished resolution, non-negligible background, challenging trigger, reconstruction, particle ID.

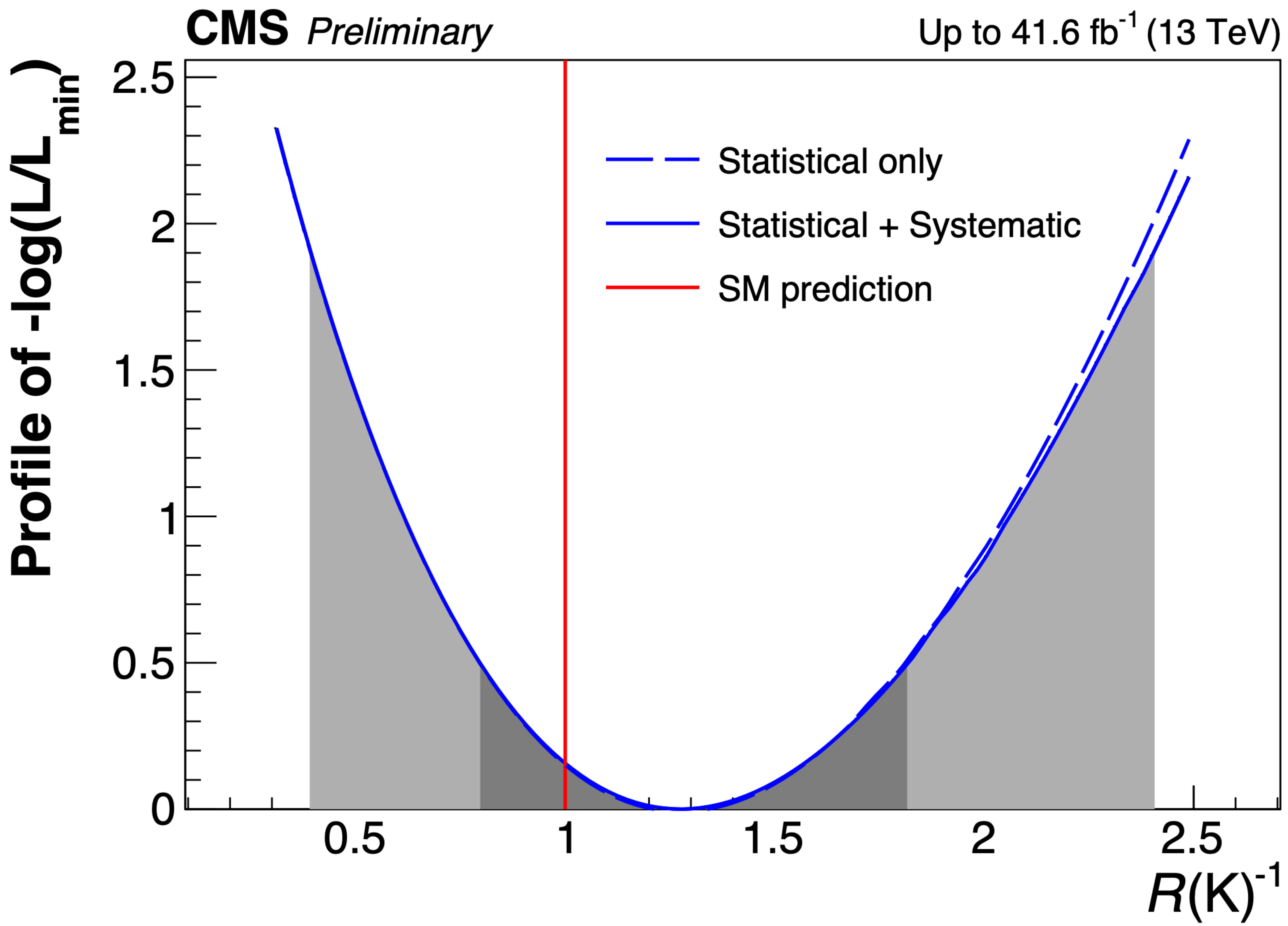

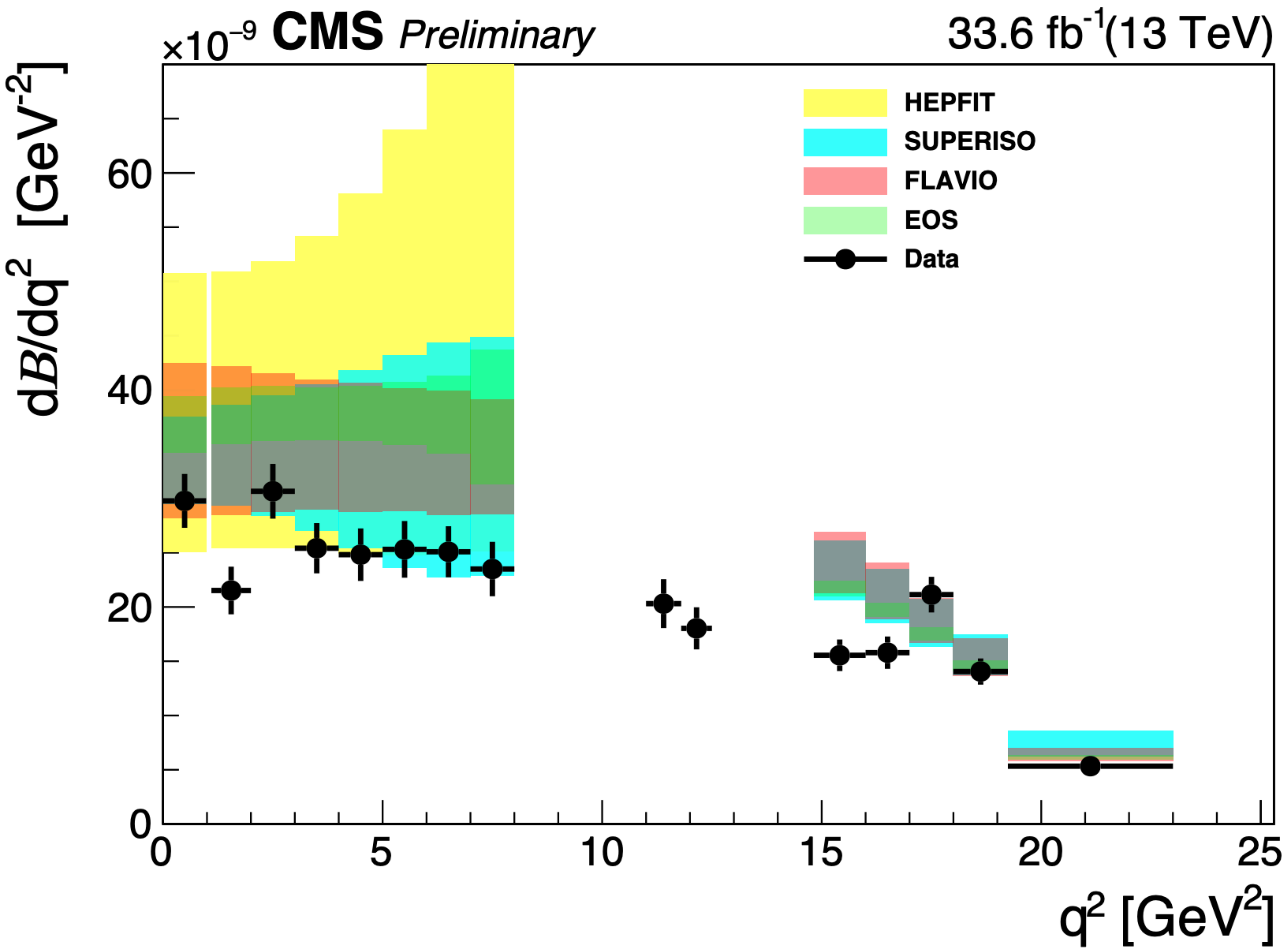

$$R(K) = 0.78^{+0.46}_{-0.23}\,(\text{stat.})\,^{+0.09}_{-0.05}\,(\text{syst.})$$

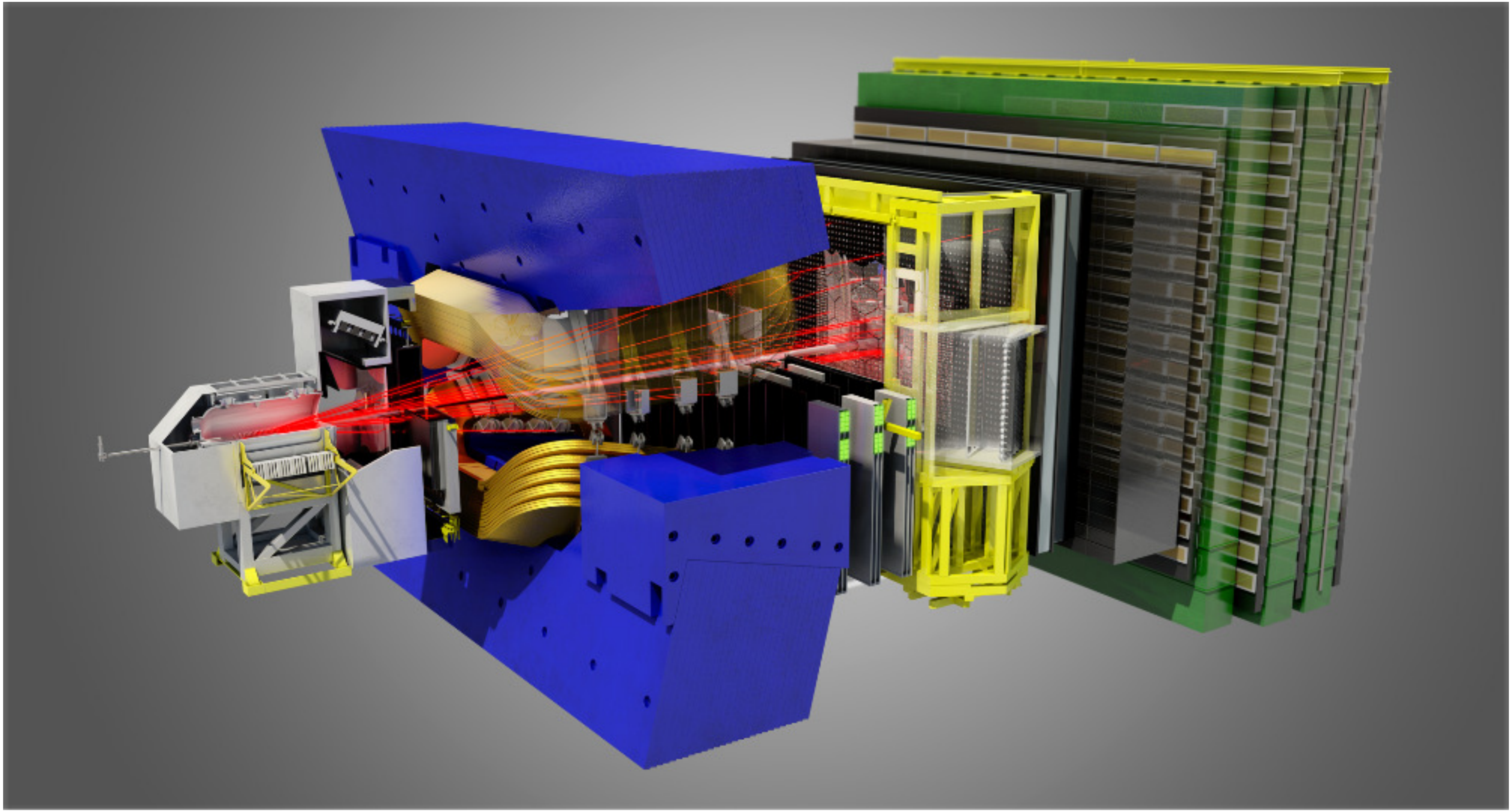

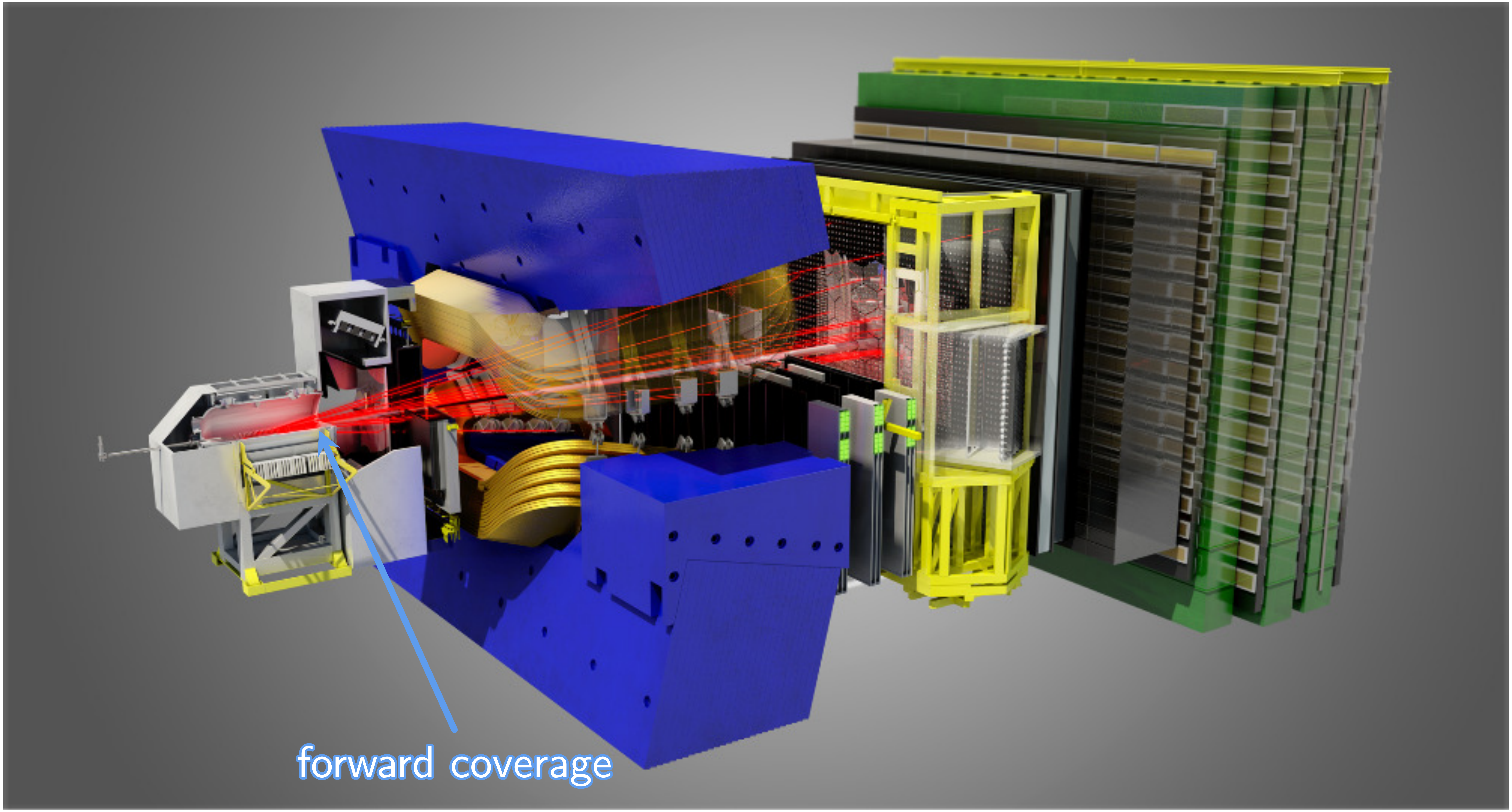

$\sigma_{b\bar{b}}$ up to $\sim 500\ \mu\text{b}$

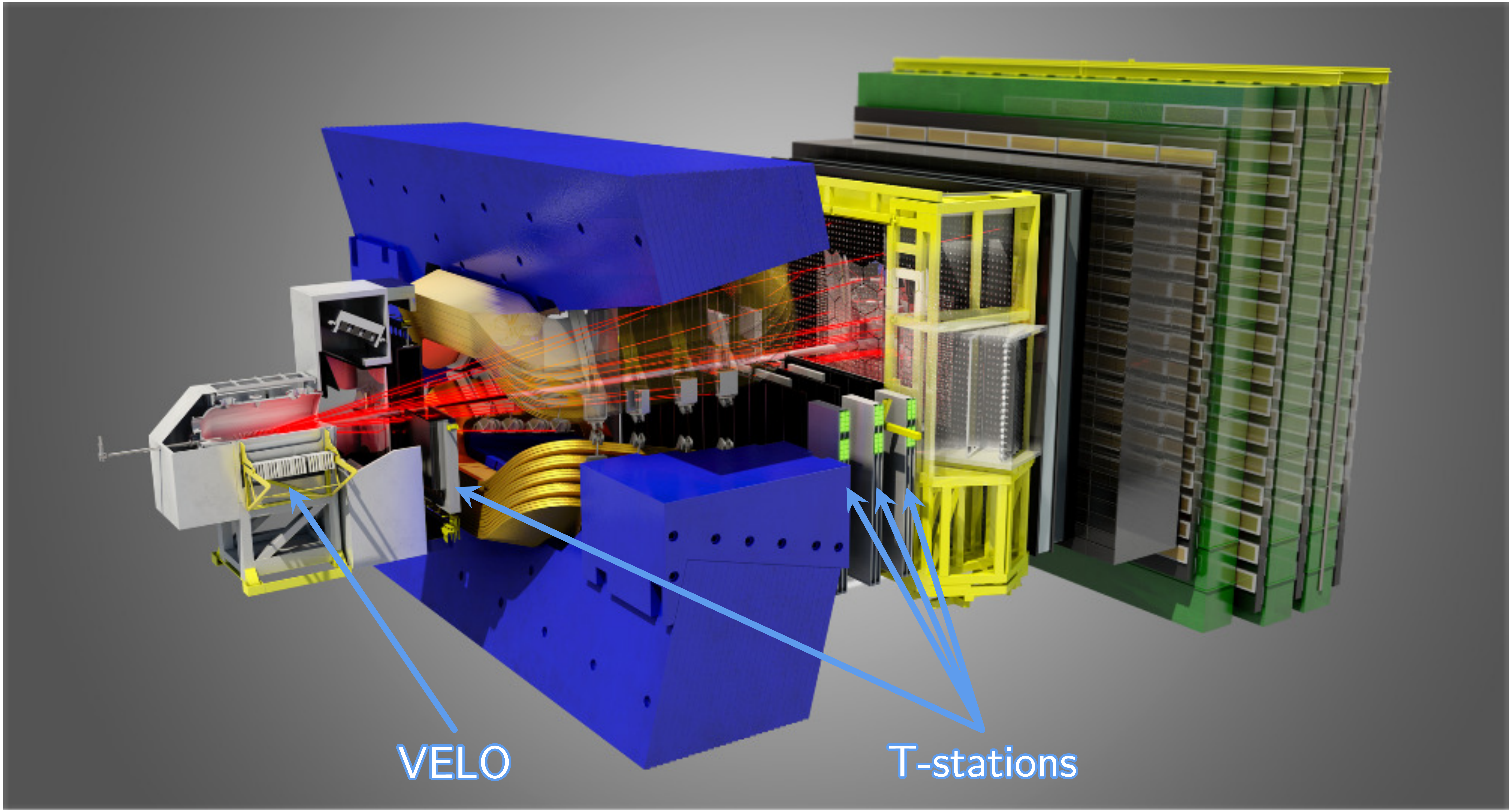

$\sigma_{\mathrm{IP}} = (15 \pm 29/p_{\mathrm{T}})\ \mu\mathrm{m} \qquad \sigma_p/p \in [0.5\%,\ 1\%]$

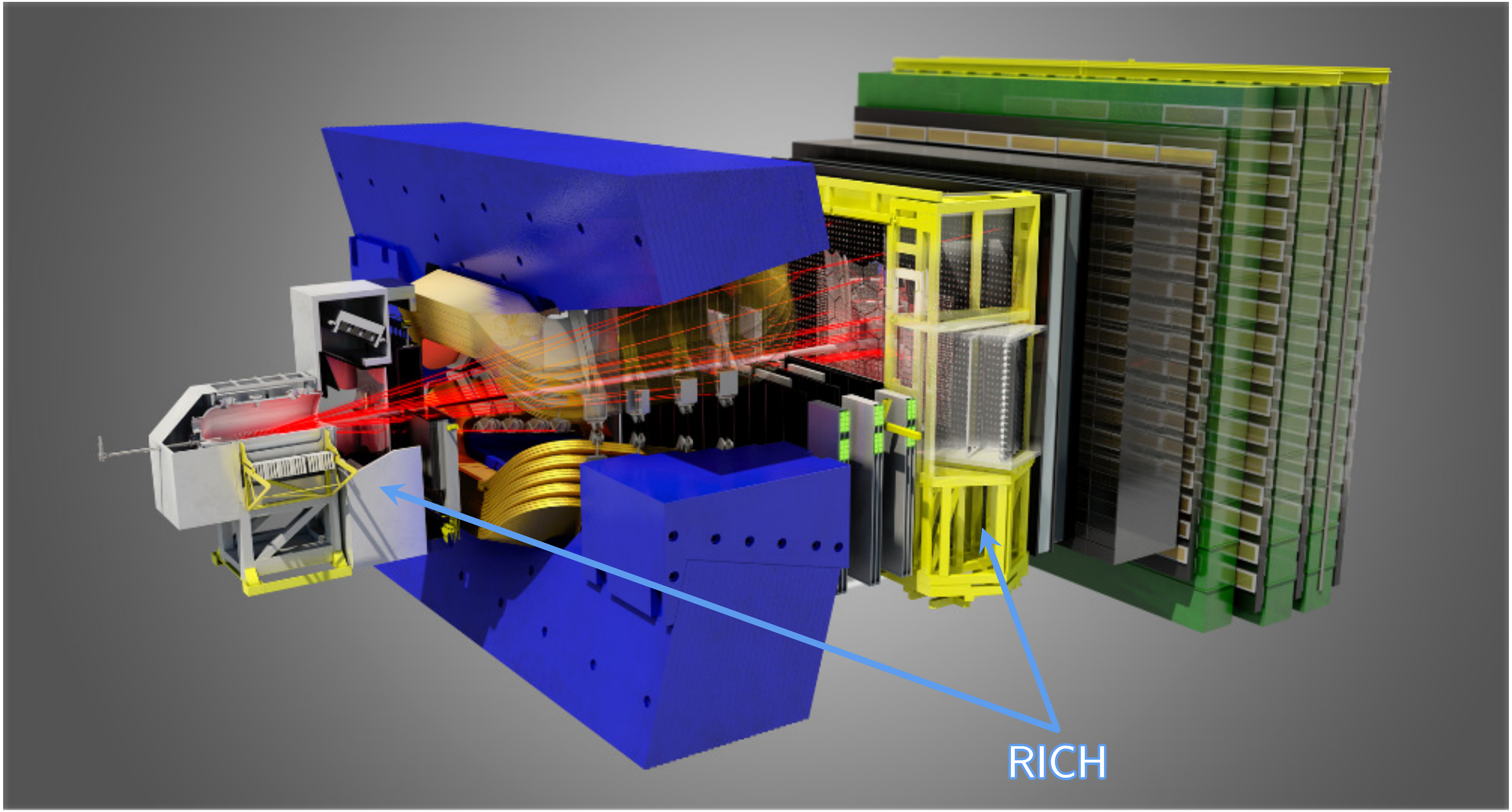

$$\varepsilon_{K\to K} \sim 95\%,\ \varepsilon_{\pi\to K} \sim 5\%$$

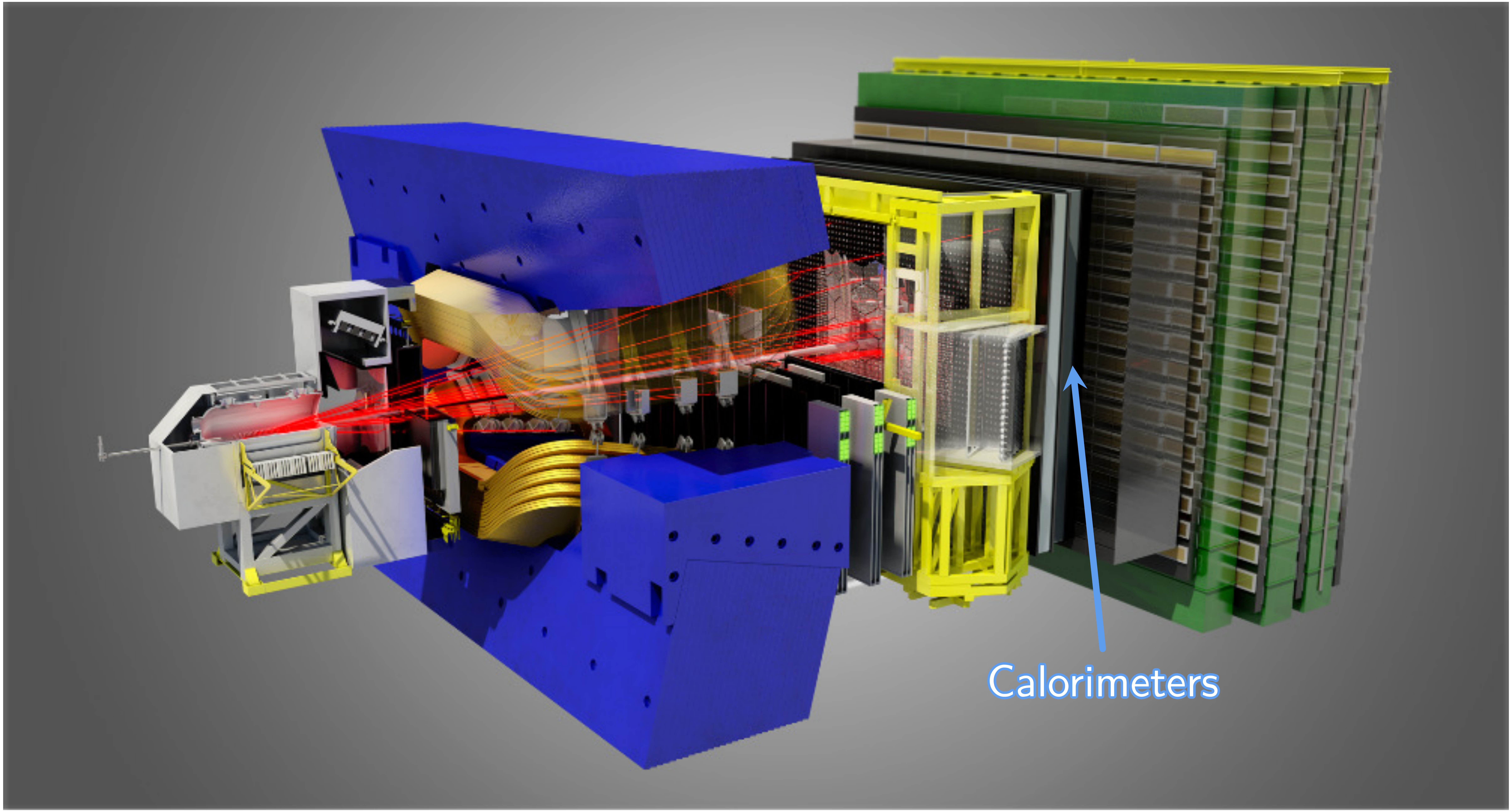

$$\sigma_E/E = 1\% + 10\%/\sqrt{E}$$

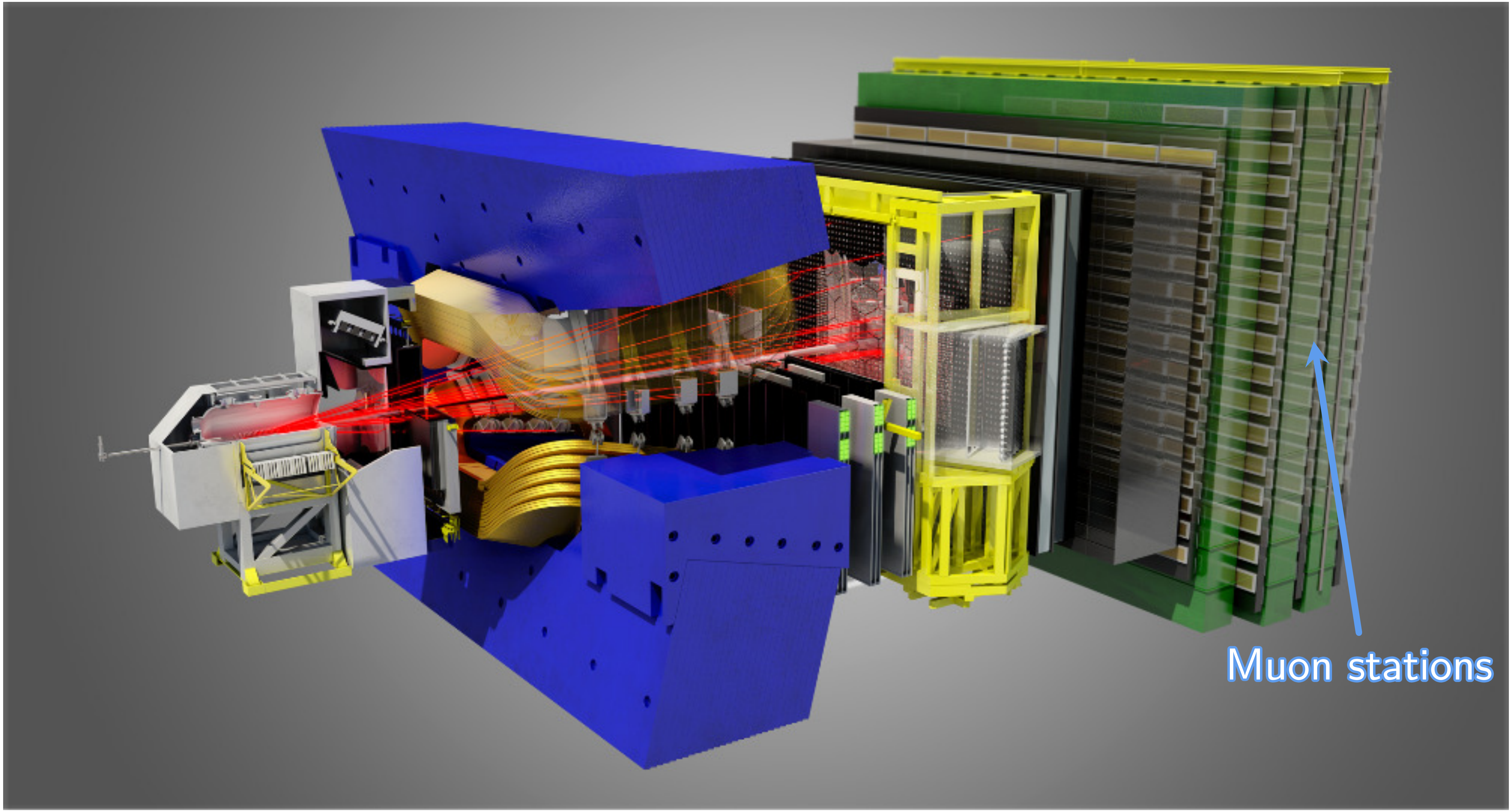

$$\varepsilon_{\mu\to\mu} \sim 97\%,\ \varepsilon_{\pi\to\mu} \sim 1-3\%$$